UNIVERSITÀ
DEGLI STUDI
DI PADOVA

Sede amministrativa: Università degli Studi di Padova

Dipartimento di **Biologia**

CORSO DI DOTTORATO DI RICERCA IN: **BIOSCIENZE E BIOTECNOLOGIE**

CURRICOLUM: **BIOLOGIA CELLULARE**

CICLO: **XXIX**

A novel model of Miller Fisher syndrome to study motor axon terminal regeneration

Tesi redatta con il contributo finanziario della Cassa di Risparmio di Padova e Rovigo

Coordinatore: Ch.mo Prof. Paolo Bernardi

Supervisore: Ch.mo Prof. Cesare Montecucco

Co-Supervisore: Dott.ssa Michela Rigoni

Dottorando: Umberto Rodella

SOMMARIO

La giunzione neuromuscolare (*neuromuscular junction,* NMJ) è una sinapsi 'tripartita', composta da un terminale assonico di un motoneurone (*motor axon terminal,* MAT), una fibra muscolare postsinaptica, e da cellule di Schwann perisinaptiche (*perisynaptic Schwann cells,* PSC). La funzionalità della NMJ è essenziale per l'esecuzione dei movimenti corporei. Tuttavia la sua anatomia la rende particolarmente esposta ad una vasta gamma di stimoli patologici, quali neurotossine animali e batteriche, sostanze tossiche, traumi meccanici e malattie autoimmuni.

Nella sindrome di Miller Fisher (*Miller Fisher Syndrome,* MFS), auto-anticorpi riconoscono specifici gangliosidi (>90% GQ1b) presenti nel MAT e attivano la cascata del complemento alla sua superficie, causandone la degenerazione. Questo danno è reversibile, in quanto il MAT è in grado di rigenerare completamente e di ristabilire la trasmissione sinaptica.

Le PSC sono tra i principali effettori della rigenerazione della NMJ. Ad oggi, tuttavia, l'attuale comprensione dei ruoli di queste cellule in questa neuropatia autoimmune è principalmente fenomenologica, e ulteriori studi molecolari.

È stato riportato che il MAT in degenerazione rilascia segnali di allarme (*alarmine*) capaci di attivare il fenotipo di pro-rigenerazione delle PSC. Dunque si può dedurre che il MAT gioca un ruolo attivo nel processo della propria degenerazione. Inoltre è probabile che molti altri segnali siano generati da parte di tutti e tre i componenti della NMJ, che generano così un network complesso di comunicazione intercellulare, il quale è stato solo parzialmente compreso.

Nel progetto di dottorato qui presentato è stato sviluppato un nuovo modello *in vivo* di MFS, allo scopo di chiarire gli eventi molecolari e cellulari che avvengono nelle PSC in seguito a danno del MAT osservato nella MFS. Ciò è stato permesso tramite l'utilizzo di FS3, un anticorpo monoclonale che riconosce gangliosidi associati alla MFS, e siero umano (*normal human serum,* NHS), utilizzato come fonte di proteine del complemento. La amministrazione subcutanea nel muscolo LAL, o intramuscolare nel muscolo soleo, della combinazione di questi due elementi induce la degenerazione del MAT, e i suoi frammenti vengono fagocitati e degradati dalle PSC. Entro pochi giorni dall'iniezione la rigenerazione del MAT è completa sia a livello morfologico che funzionale, come evidenziato da analisi di immunofluorescenza ed elettrofisiologiche. Gli effetti osservati sono strettamente dipendenti dall'anticorpo e dal sistema del complemento, in quanto non viene osservata neurodegenerazione in assenza di FS3 o quando il NHS viene inattivato al calore.

Allo scopo di identificare le *alarmine* neuronali responsabili dell'attivazione delle PSC e le conseguenti risposte molecolari di quest'ultime, è stato parallelamente sviluppato un modello *in vitro* di MFS, che consiste nell'esposizioneì della combinazione di FS3 e NHS (FS3+NHS) a colture primarie di neuroni cerebellari o di motoneuroni da midollo spinale. Ciò causa un'entrata massiccia e incontrollata di calcio (Ca^{2+}) a livello dei neuriti, associata alla formazione di protuberanze, o *bulges*, a livello dei neuriti stessi. Questi *bulges* sono siti di accumulo di mitocondri gonfi e disfunzionali, e di produzione di perossido di idrogeno (H_2O_2). Il perossido di idrogeno è un segnale di allarme per le cellule di Schwann (*Schwann cells*, SC). Infatti in co-colture di neuroni e SC, il H_2O_2 derivante dai neuroni attaccati da FS3+NHS induce l'attivazione nelle SC del pathway di ERK1/2, conosciuto per il suo importante ruolo di induzione del fenotipo pro-rigenerazione delle SC.

Inoltre, tramite il modello *in vitro* di MFS, è stata identificata una seconda *alarmina* coinvolta nell'attivazione delle SC, l'adenosina trifosfato (ATP).

Infatti, neuroni primari esposti al complesso FS3+NHS rilasciano nel mezzo extracellulare ATP, che a sua volta induce oscillazioni intracellulari di Ca^{2+} nelle SC. Queste oscillazioni sono abolite in presenza di apirasi, un enzima che degrada l'ATP, nel mezzo di incubazione.

In aggiunta, esperimenti con un sensore FRET per l'AMP ciclico (cAMP) hanno mostrato che i livelli di SC aumentano in co-colture di neuroni e SC in seguito al danno neuronale esercitato da FS3+NHS. All'aumento di cAMP intracellulare osservata ne consegue un'aumentata fosforilazione (ovvero attivazione) del fattore di trascrizione CREB (*cAMP response element-binding protein*), anch'essa ATP-dipendente.

In conclusione, il lavoro svolto in questo progetto di dottorato ha portato allo sviluppo di nuovo modelli *in vivo* e *in vitro* di MFS. Questi sono stati utilizzati per lo studio della comunicazione molecolare tra il MAT e le PSC. Il perossido di idrogeno e l'ATP sono stati identificati come importanti *alarmine* neuronali, capaci di attivare il fenotipo pro-rigenerazione delle SC.

Crediamo che questi risultati contribuiscano a gettare luce sugli eventi molecolari e cellulari che avvengono alla NMJ nella MFS, e che queste conoscenze possano venire estese anche ad altre patologie che affliggono il MAT.

SUMMARY

The neuromuscular junction (NMJ) is a 'tripartite' synapse, composed of the presynaptic motor axon terminal (MAT), the muscle fiber and perisynaptic Schwann cells (PSCs). NMJ functionality is essential for the execution of body movements and it is anatomically exposed, becoming an easy target of bacterial and animal neurotoxins, toxic chemicals, mechanical trauma, and autoimmune diseases.

In the Miller Fisher Syndrome (MFS) autoantibodies against specific gangliosides (>90% GQ1b) bind to MAT and in turn activate the complement system cascade at its surface, leading to nerve degeneration. Such damage is reversible, as the motor neuron is able to fully regenerate and restore neurotransmission.

PSCs are main supporters of NMJ regeneration: to date, however, the current understanding of PSCs role in this autoimmune neuropathy is mostly phenomenological, and molecular studies are needed. It was recently reported that the degenerating MAT release alarm signals (*alarmins*) able to activate the pro-regenerating phenotype of PSCs. Therefore, MAT can be considered an active player of its own regeneration. In addition, many other signals are thought to be generated by all the three main components of the NMJ, thus generating a complex inter-cellular communication network, which has been only partially identified.

In order to better elucidate the molecular and cellular events driving PSCs response to MAT damage in MFS, we recently developed a novel *in vivo* MFS model. The combination of FS3, a monoclonal antibody against gangliosides related to MFS, and normal human serum (NHS) as a source of complement, administered subcutaneously in LAL muscles and intramuscularly in soleus muscle in mice, causes the degeneration of MAT. Soon after MAT destruction, neuronal debris are engulfed and digested by PSCs. Within few days after injection MAT regrowth is morphologically and functionally complete, as assessed by immunofluorescence analysis and electrophysiological recordings. The effect is antibody- and complement-dependent, as no MAT degeneration takes place in the absence of FS3, nor when NHS is heat-inactivated.

To identify the neuronal *alarmins* responsible for PSCs activation and the signaling pathways engaged, we have parallely set up an *in vitro* MFS model consisting of administration of FS3 plus NHS to primary cerebellar neurons and spinal cord motor neurons, which causes a complement-dependent massive Ca^{2+} overload in neurite, together with the formation of neurite enlargements,

named bulges. Bulges are sites of accumulation of swollen and dysfunctional mitochondria, and of localized hydrogen peroxide (H_2O_2) production. Hydrogen peroxide is an alarm signal for SCs. Indeed, in FS3 *plus* NHS attacked neurons-SCs co-cultures, neuron-derived H_2O_2 induces activation of the ERK1/2 pathway in SCs, a known crucial player of the switch toward a pro-regenerative phenotype of SCs.

In addition, we identified adenosine triphosphate (ATP) as an additional *alarmin* involved in SCs activation. Indeed, primary neurons exposed to FS3 plus NHS release ATP in the extracellular medium, which in turn evokes intracellular calcium spikes within SCs in co-cultures with neurons. These spikes were significantly abolished in the presence of the ATP-inactivating enzyme apyrase in the incubation medium.

Furthermore, experiments with a FRET-based cyclic AMP (cAMP) sensor show that, upon FS3 *plus* NHS addition in neurons-SCs co-cultures, cAMP levels rise in SCs, and this event eventually results in an ATP-dependent increased phosphorylation the transcription factor CREB (cAMP response element-binding protein).

In conclusion, the work performed during this PhD project has led to the development of novel *in vitro* and *in vivo* models of MFS, in order to study the molecular communication between MAT and PSCs. Hydrogen peroxide and ATP were found to be important neuronal *alarmins*, able to activate pro-regenerative pathways within SCs.

We believe these results throw light on the molecular and cellular events taking place in MFS, and may well be extended to other MAT affecting pathologies.

TABLE OF CONTENTS

1. INTRODUCTION

1.1. The Neuromuscular junction: structure and physiology

The neuromuscular junction (NMJ) is the specialized anatomical structure of the peripheral nervous system (PNS) which allows, triggers, and regulates muscle contraction. It is therefore a master manager of body movements: it represents an essential link between decision makings carried out at the level of the central nervous system (CNS) and order executions fulfilled by skeletal muscles. This highly specialized synapse consists of three main components: the motor axon terminal (MAT), the skeletal muscle fibre (MF), and perisynaptic Schwann cells (PSCs) (*peri-*, from Ancient Greek περί, stands for *surrounding* or *around*), also termed terminal Schwann cells (TSCs).

MATs are the ultimate output of motor neurons, whose cell bodies lie in the spinal cord. MATs primary physiological function is the conversion of the electrical signal travelling along the axon into a chemical one directed to MF. This goal is achieved by active packaging of small vesicles, the synaptic vesicles, inside the MAT, in close proximity to the plasma membrane facing the MF, termed the presynaptic membrane. The MF counterpart of the presynaptic terminal is named postsynaptic membrane. Acetylcholine (Ach), a small molecule neurotransmitter, is stocked inside synaptic vesicles. Once the action potential (the electrical signal) coming from the axon reaches the MAT, it triggers a rapid sequence of events leading to the transient rise of intracellular calcium concentration ($[Ca^{2+}]i$), which in turn induces the fusion of synaptic vesicles with the presynaptic membrane, and the release of their content into the space separating the presynaptic membrane to the postsynaptic one, named synaptic cleft. Ach molecules can now freely reach the postsynaptic membrane, highly enriched in nicotinic acetylcholine receptors (AchRs) which, upon Ach binding, initiate the intracellular transduction pathway which eventually leads to muscle contraction.

A multi-cellular carpet of PSCs covers the space close to MAT-MF contact. Schwann cells (SCs) are the principal glia cells of the PNS: myelinating SCs wrap motor neuron axons and participate in the conduction of nervous impulses along nerves, and non-myelinating SCs, involved in maintenance of smaller axons. PSCs belong to non-myelinating SCs and represent a specialized subtype of the

NMJ: there are typically 3-5 PSCs/NMJ in mammalians, depending to the NMJ size (1). Their function(s) in physiological and pathological conditions will be discussed in the next chapters.

1.2 Perisynaptic Schwann cells: key regulators of NMJ formation and activity

PSCs have been considered merely passive players in NMJ functions for a long time: on the contrary, beside the role of maintaining a proper environment for MAT and electrically sealing the synaptic cleft, PSCs fulfil a number of crucial tasks in physiological as well as pathological conditions.

Firstly, they participate in NMJ formation: during embryonic development SCs precursors, which originate from neural crest cells (2), co-migrate with the developing motor axons toward the muscle, and are hence present at the earliest nerve-muscle contact, suggesting an involvement in neuromuscular synapse formation (3). Further evidence comes from observations from murine models in which Neuregulin-1 / erbB signalling was disrupted. This pathway is essential for the survival of the entire SC lineage (including PSCs), and its disruption causes the lack of SCs. These studies led to the conclusion that SCs are dispensable for the initial nerve-muscle contacts, but are essential for subsequent growth and maintenance of the developing synapses. Indeed in absence of SCs NMJs are initially established but fail to be maintained, with extensive motor neuron death (2). This observation has been further confirmed by experiments at the developing NMJ in tadpoles, in which SCs processes always precedes AchRs deposition and synaptic growth, thus appearing to guide nerve terminals growth (4).

The privileged position of PSCs at the adult NMJ allows them to actively participate also to the regulation of synaptic activity. Indeed, they express several transmembrane receptors for neurotransmitters such as Ach, adenosine, and adenosine triphosphate (ATP). Pioneer studies have demonstrated that high frequency stimulation of the motor nerve causes a rapid elevation of $[Ca^{2+}]i$ in PSCs in amphibian NMJs. This was dependent on Ach and ATP released by MAT during nerve activity (5). The consequent G-protein activation of PSCs leads to production of molecules that modulate synaptic output, providing an important feedback regulation of the synapse in response to MAT activity.

Furthermore, the ability of PSCs to sense and modulate synaptic transmission observed in the frog NMJ have been convincingly replicated also at mammalian NMJ (6), indicating that synapse-glia intercellular communications are a fundamental, evolutionarily conserved feature of the NMJ.

1.3 Schwann cells functions in neuro-degeneration and regeneration: the classical *cut and crush* approach

A number of high debilitating neurodegenerative diseases affects the PNS such as amyotrophic lateral sclerosis, myasthenia gravis and Guillain-Barré syndromes. Some of them are incurable, or treatments are only partially effective. There is therefore an urgent need of novel knowledges in this field, to unravel the molecular mechanisms underlying degeneration and regeneration of peripheral neurons, and how the cross-talk between peripheral neurons and other cells (muscle cells, SCs, immune cells) contribute to such process.

The traditional experimental approach for studies on nerve degeneration and regeneration consists in the induction of a mechanical trauma either by transection or by crushing of the nerve (*cut and crush* method). Upon such insult the segment of the motor axon distally to the injury degenerates in a process called Wallerian Degeneration. First described by Augustus Waller in 1850 (7), this complex array of events usually begins within 24-36 hours from the lesion, when failure of synaptic transmission and muscle denervation occur. Alterations of axonal membrane permeability cause an increase in $[Ca^{2+}]i$ and the consequent activation of Ca^{2+}-dependent proteases, which lead to disintegration of axonal cytoskeleton and organelles, together with axolemma swelling and accumulation of swelled mitochondria (8).

A complex response to axonal injury rapidly begins: myelinating SCs de-differentiate to a progenitor-like state, becoming “reactive”, and start proliferating (9). They undergo a radical change in gene expression, down-regulate structural proteins (such as the protein zero P0, the myelin basic protein MBP and the myelin associated glycoprotein), and up-regulate cell-adhesion molecules and growth factors (10). Interestingly, they acquire phagocytic-like activities, and start clearing up axonal debris. They also recruit macrophages and other immune cells by releasing cytokines and chemokines, thus improving the clearing rate favouring regeneration (11). Importantly, SCs also guarantee structural support to the regenerating motor axon: during their proliferation phase, SCs begin to form a line of cells called Bands of Bungner,

along which axons regenerate in close association toward the proper direction, i.e. the NMJ (12).

1.4 PSCs roles in NMJ pathological conditions

PSCs plasticity in pathological conditions affecting the NMJ is really remarkable. As NMJ lies outside the blood-nerve barrier (BNB), it is anatomically exposed (13) and an easy target of many bacterial and animal neurotoxins, toxic chemicals, mechanical trauma, and autoimmune diseases. It is therefore an urgent evolutionary requirement for the body to rapidly restore NMJ functionality upon motor nerve injury. Noteworthy, differently from central neurons, peripheral neurons have the intrinsic ability to repair after nerve injury (14). Upon MAT injury PSCs undergo to an array of responses very similar to myelinating SCs during Wallerian degeneration, de-differentiating and re-entering into the cell cycle. They acquire phagocytic activity and contribute to the removal of debris coming from degenerating MAT.

A boost in the research on PSCs biology came from the work of Son and Thompson in 1995. Upon full denervation of rat soleus muscle by nerve crush, the authors observed that PSCs extend processes (also called sprouts) which form a network interconnecting denervated NMJs. Moreover, sprouts extend towards the cut ends of the severed axons, and are in turn employed as guide/substrate for axon regrowth toward the NMJ (15). It was demonstrated for the first time that PSCs are crucial for MAT regeneration, guiding reinnervating axons toward the original NMJs. Interestingly, paralysis by botulinum neurotoxins, which preserve MAT structural integrity, also causes PSCs sprouting from the NMJ, together with MAT sprouting associated with PSCs processes (16). In line with this, PSCs can sense neurotransmission and respond to denervation and/or presynaptic blockade by changing their gene expression (17).

In summary, in absence of appropriate signals from the MAT PSCs, similarly to myelinating SCs during Wallerian degeneration, undergo a complex array of transcriptional, biochemical and morphological changes functional to neuroregeneration.

1.5 α-Latrotoxin: an innovative tool to study NMJ degeneration and regeneration

Much of our knowledge on the processes of neuro-degeneration and regeneration comes from in *vivo* studies based on the *cut and crush* of the nerve. However, this approach introduces some drawbacks, the most important being the induction of Wallerian. Indeed, Wallerian degeneration sets in motion a complex battery of events involving, besides SCs, many different cell types, mainly macrophages and other immune cells, with a pronounced inflammatory response all along the degenerating nerve segment distal to the cut or crush site. This implies that: i) the *cut and crush* model only partially overlaps with those neurological disorders affecting predominantly the NMJ, such as amyotrophic lateral sclerosis, Miller Fisher syndrome and other Guillain Barré syndrome subtypes; ii) it cannot be reproduced by simplified *in vitro* models; iii) the role of PSCs in the restoration of NMJs cannot be discerned from that of myelinating SCs and of inflammatory cells.

Taking in account these considerations, we have recently developed an innovative experimental approach, alternative to the surgical *cut and crush* model, based on the use two animal neurotoxins acting at the NMJ (18).

In particular, α-Latrotoxin (α-LTX), a pore-forming toxin from the venom of black widow spiders (genus *Latrodectus*), represents a reliable tool for a better understanding of PSCs role in MAT regeneration (18). Its effect is indeed very specific for the MAT and highly reproducible.

In the venom of black widow spider α-LTX is a monomer. Once bound to its receptors at the presynaptic membrane it inserts in the lipid bilayer and tetramerizes, forming a 10 Å diameter channel across the membrane, which permits a massive influx of water and ions, mainly Ca^{2+}, inside the MAT (19). This uncontrolled $[Ca^{2+}]i$ rise triggers a massive neuroexocytosis followed by progressive degeneration of the MAT due to activation of Ca^{2+}-dependent proteases, mainly calpains, which carry out cytoskeletal and organelle degradation (18,20).

Electrophysiological recordings of murine muscle-nerve preparations intoxicated with α-LTX show a rapid increase in the frequency of spontaneous miniature postsynaptic potentials (MEPPs), due to the massive neuroexocytosis, followed by the complete inhibition of evoked action potentials (EPPs) induced by MAT destruction. Importantly, the resulting skeletal muscle paralysis is reversible: MAT regeneration and NMJ re-innervation are completely restored in mice in 4 to 8 days (18,20).

Electron microscopy studies show that in the earliest stages of intoxication MATs become markedly swollen and depleted of synaptic vesicles. Mitochondria appear also swollen and rounded (20).

The abovementioned morphological and electrophysiological effects of α-LTX action at murine NMJs were also observed in murine models of Miller Fisher syndrome, an autoimmune disease targeting the NMJ (21), suggesting that the molecular mechanisms underlying α-LTX-dependent MAT destruction, as well as PSCs pro-regenerative response(s) leading to MAT reconstruction, may be shared by other NMJ-affecting diseases.

In addition, α-LTX can be used in simplified *in vitro* models. Indeed, intoxication of primary cultured neurons with α-LTX largely recapitulates α-LTX effects at NMJ, i.e. large calcium influx, formation of swellings along neurites, called *bulges*, hallmarks of massive neuroexocytosis, calpains activation and cytoskeletal degradation (22,23).

These *in vitro* models are advantageous for their vulnerability and simplicity. In addition, primary neurons/SCs co-cultures can be set up to mimic the intimate relationships between MAT and PSCs.

Summarizing, α-LTX represents an innovative tool to induce an acute, confined and reversible MAT degeneration without inflammation, to monitor the subsequent regeneration and define PSCs contribution to such process.

1.6 MAT as active player of its own regeneration: the concept of *alarmins*

By applying the '*molecular model*' of neuro-degeneration and regeneration, i.e. *in vivo* intramuscular acute administration of α-LTX in mice, our laboratory has recently uncovered some of the intercellular events leading to neuroregeneration after MAT damage.

Upon MAT α-LTX dependent destruction, PSCs start to display pro-regenerative activities. They engulf nerve debris, eventually clearing the NMJ from pieces of destroyed MAT, and sprout processes, along which axon stump can regrow toward the denervated NMJ (18).

Degenerating neurons have an active role in their own regeneration by activating neighbouring SCs. This can be achieved by an active release of molecules in the extracellular environment which alert PSCs, hence termed *alarmins* (18,24).

Damage-associated molecular patterns (DAMPs) are *alarm* molecules often released from cells in a number of patho-physiological conditions associated to cell death and injury. Normally present inside the cell in different subcellular compartments, once liberated in the extracellular milieu, DAMPs are recognized by the innate immune system by pattern recognition receptors (PRRs) and activate an inflammatory response, acting as chemotactic, pro-phagocytic and immunostimulatory factors (25).

Upon nerve damage SCs acquire phagocytic properties and play important roles in the modulation of immune response, producing and secreting a wide variety of proinflammatory cytokines, such as IL-1β, IL-6, TNF-α, TGF-β. These chemoattractants induce the invasion of immune cells to the site of injury, further contributing to the removal of axon debris (26).

SCs also express Toll-like Receptors (TLRs), a subfamily of PRRs, mostly found in immune cells and, in addition, they act as antigen-presenting cells by expression of MHC class II at their surface (27,28).

These data strongly suggest that SCs can be considered, under certain conditions, immunocompetent cells and can sense and be activated by DAMPs.

Experiments performed in our laboratory found indeed a number of *alarmins* released by the damaged MAT which were able to induce activation of pro-regenerative signaling pathways in PSCs. Among these, hydrogen peroxide (H_2O_2), mitochondrial DNA and adenosine triphosphate (ATP) appear to be major PSCs activators (18,24).

H_2O_2 is themost stable among reactive oxygen species (ROS). For long time believed solely harmful molecules, accumulating evidence show that ROS, particularly H_2O_2, can also be important second messengers in many intra- and inter-cellular pathways. H_2O_2 main source are cellular respiration and oxidative phosphorylation within mitochondria, where the short-lived superoxide ($O_2^{\bullet-}$) is converted to H_2O_2 by superoxide dismutases. The relative stability and uncharged nature of H_2O_2 permits its diffusion across long distances and membranes, possibly acting as a paracrine signal (29,30). Indeed, MAT exposed to α-LTX produce mitochondrial H_2O_2, which in turn activates ERK1/2 signalling pathway in neighbouring PSCs. This pathway was previously shown to play a crucial role in orchestrating nerve repair (31), stimulating SCs pro-regenerative features. Accordingly, administration of catalase (a H_2O_2-inactivating enzyme), as well as a ERK1/2 pathway inhibitor, significantly impaired MAT regeneration and muscle reinnervation after α-LTX dependent neurodegeneration (18).

In addition to H_2O_2, also mitochondrial DNA (partly via exosome release), cytochrome C, and ATP have been observed to be released by α-LTX intoxicated neurons and act as *alarmins* able to activate Schwann cells (18,24). These results throw light on the wide range of intracellular mechanisms that contributes to transmit the damage signal to the surrounding Schwann cells, preparing them for the complex processes that support neuroregeneration. ATP in particular is an extracellular messenger in many tissues and cell types. Beside its known role of energy source, it acts on different purinergic receptors expressed in the plasma membrane of nearly all cell types and tissues. Purinergic engagement can activate different pathways in the cell, including $[Ca^{2+}]i$ modulation and cyclic adenosine monophosphate (cAMP) synthesis (32,33).

ATP is well-known to play a role in the chemical communication between MAT and PSCs during physiological conditions of the NMJ (5,34). Pharmacological blockade of the purinergic signalling impaired axonal regeneration in a model of rat nerve transection (35), suggesting a role in intercellular communication also during pathological conditions.

Accordingly, *in vitro* experiments with α-LTX provided evidence of an early release by degenerating neurons of ATP. It contributes to the activation of a series of intracellular pathways within SCs that are crucial for nerve regeneration: Ca^{2+}, cAMP, CREB (cAMP response element-binding protein), and ERK1/2 (24).

In summary, the toxin model allowed us to shed light on the molecular cross-talk between degenerating MAT and nearby cells, pointing out the role of H_2O_2 and ATP as prominent neuron-derived *alarmins*, leading to the activation of pro-regenerative signalling pathways in SCs.

1.7 α-Latrotoxin and Miller Fisher syndrome: do common pathogenic steps trigger common regenerative mechanisms?

We decided to extend the study on the cross-talk among degenerating MAT and PSCs to other NMJ-affecting disorders, such as the Miller Fisher syndrome (MFS).

MFS is a subtype of Guillain-Barré syndrome (GBS). In MFS the main toxic stimulus is represented by a pore-forming complex assembled at the presynaptic membrane, whose pathological effects at MAT are Ca^{2+}-dependent, morphologically and electrophysiologically akin to those of α-LTX (see next chapters) (21). PSCs phagocytosis with removal of nerve debris occurs also in animal models of MFS (36).

We therefore speculated that during MFS the inter-cellular communication between MAT and PSCs may be closely similar to that occurring at α-LTX-poisoned NMJs.
An introduction to GBS and MFS, as well as details about pathogenesis and consequences for NMJ, are presented below.

1.8 Guillain-Barré syndrome: historical background and clinical traits

Firstly described in 1916, the Guillain-Barré syndrome (GBS) takes its name from two military doctors, Georges Guillain and Jean-Alexandre Barrè, who made the first clinical observations on two soldiers of the French Army who had become partially paralysed during the First World War. One, in particular, had fallen over when he put his pack on and had been unable to get up. In the original paper, which they published together with the physiologist Andrè Strohl, they asserted:

"*These two patients, without a detectable cause, developed a clinical syndrome characterized by disorders of all muscles of the upper and lower limbs, worse distally, the loss of tendon reflexes, with preservation of cutaneous reflexes, paresthesia with mild disorders of objective sensation, pain when pressure was applied to muscle masses, small modifications of the electric reactions of nerves and muscles and the distinct finding in the cerebrospinal fluid of a marked hyperalbuminosis without cytological reaction*" (37).

The cause of the condition was left unanswered, assumed to be some unknown kind of infection or poisoning. Both soldiers quickly recovered.
In 1956 Charles Miller Fisher, a Canadian neurologist, described three patients with acute external ophthalmoplegia (eye movements paralysis), ataxia (lack of voluntary coordination of muscle movements) and areflexia (absent tendon reflexes). Two patients had no weakness; the other had a facial palsy and possible weakness. None of the three patients had limbs paralysis. All three recovered spontaneously (38).
Because some patients with GBS had ophthalmoplegia and other clinical similarities, Miller Fisher concluded that these patients had suffered a disorder akin to GBS.
Nowadays the three clinical symptoms observed by Miller Fisher, i.e. ophthalmoplegia, ataxia and areflexia, are the clinical triad marking the MFS. MFS is now considered one GBS subtype.
Indeed, GBS encompasses a group of autoimmune neuropathies, commonly characterized by acute flaccid areflexic (or hyporeflexic) paralysis with a progressive course, usually starting from

distal limbs and ascending to proximal limbs. Maximal severity is usually reached within 4 weeks from onset (39).

The different GBS subtypes display a different distribution of weakness in the limbs or in cranial-nerve innervated muscles, and can have highly different prognosis, ranging from spontaneous complete recovery (as for MFS) to a poorer outcome (40). Indeed, even though GBS is considered a reversible disease, with recovery in most cases, there is a high variation in the rate and extent of rehabilitation: the disease progression is followed by a plateau ranging from 2 days to 6 months before patients start to recover (39). Two thirds of patients are unable to walk independently when maximum weakness is reached. Approximately 20% of cases lead to total paralysis and thus to respiratory insufficiency, requiring prolonged intensive therapy with mechanical ventilation (41). Major complications including pneumonia, sepsis, pulmonary embolism, develop in 60% of intubated patients. Twenty percent of patients remain severely disabled, and 5% die (40). Additionally, GBS presents common occurrence with a yearly incidence rate between 1.1 and 1.8 per 100.000 (42), and thus represents the most frequent cause worldwide of flaccid paralysis.

Together, these observations make GBS a high social and economic burden, and one of the serious emergencies in neurology.

1.9 Pathogenesis of GBS: auto-antibodies against gangliosides are produced through molecular mimicry

GBS is a post-infectious disorder. Antecedent infections, mainly of the upper respiratory and gastrointestinal tracts, precede up to 70% of cases reported (42). The most frequently identified infectious agent associated with subsequent development of GBS is the Gram-negative *Campylobacter jejuni*, with 30% of GBS cases attributed to *C.jejuni* infection (0.65 per 1000 cases of infection), followed by cytomegalovirus (up to 10%). Other infectious agents with a well-defined relationship to GBS are: Epstein Barr virus, Varicella Zoster virus, and *Mycoplasma pneumonia* (40).

The apparent lack of correlation between precedent infections in GBS and the neuromuscular paralysis that characterize the disease can be dismissed considering the most important serological hallmark of GBS: pathological auto-antibodies in patients' sera. Indeed, microbial infections engage a host immune response (both innate and adaptive), with production of

antibodies, mainly immunoglobulin M (IgM) and G (IgG) isotypes, specific for different microbial epitopes. In GBS the adaptive immune system generates also a pool of transient serum IgG antibodies against microbial glycan epitopes, which still contribute to fight the infection but, on the other hand, cross-react with plasma membrane components of peripheral nerves (43). This pathogenic mechanism is termed *molecular mimicry*. The most known and studied molecular mimicry in the field of GBS is the one between *C.jejuni* lipo-oligosaccharide (LOS) and lipo-polysaccharide (LPS) epitopes and gangliosides of the outer leaflet of host neuronal membranes. Undoubted demonstration of the occurrence of a molecular mimicry in different subtypes of GBS, ranging from acute motor axonal neuropathy (AMAN) to MFS, was given by pioneering studies of Dr. Yuki and colleagues: animal models inoculated with *C.jejuni* LOS or heat-inactivated *C.jejuni* lysates produced IgG antibodies against gangliosides and/or developed GBS-like symptoms (44-46).

Gangliosides are glycosphingolipids composed of a hydrophobic ceramide tail attached to one or more sugars (hexoses), and containing one or more sialic acid (N-acetylneuraminic acid) linked to an oligosaccharide core (40). Their nomenclature was proposed by Svennerholm in 1994 (47): it designates a ganglioside as GXyz, where G indicates 'ganglioside', X represents the number of sialic acid molecules (M, one; D, two; T, three; Q, four), y indicates the length of the neutral sugar sequence (defined as 5 minus the number of residues), and z indicates the isomeric form, reflecting the position(s) and linkage(s) of the sialic acid residues (a, b or c) (Fig. 1).

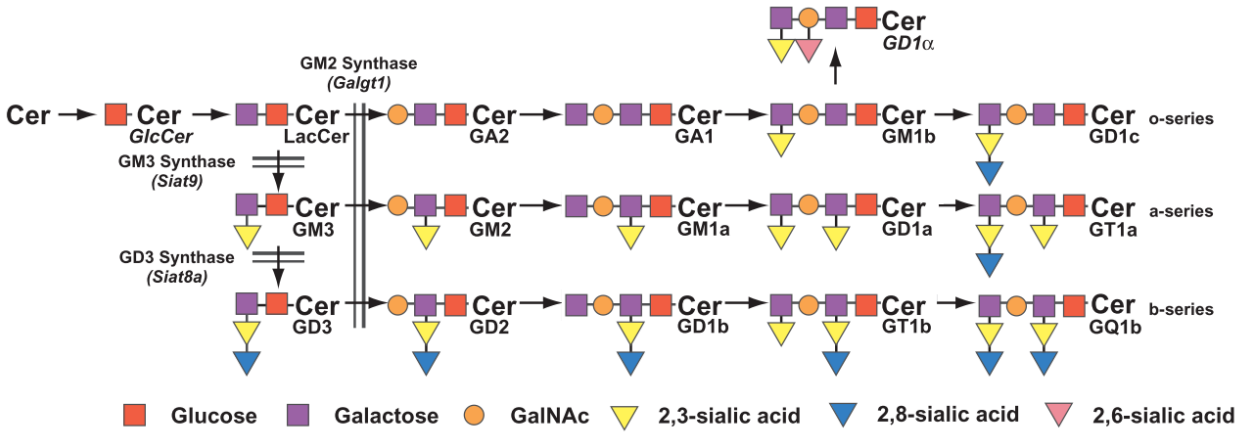

Figure 1: The ganglioside biosynthesis pathway. Key gangliosides occurring on neurons in adult mammalian brain (adapted from *Proia, 2004, Nature Genetics*).

Gangliosides are ubiquitously expressed throughout the body and are highly enriched in neurons. They represent 10–20% of the total lipid content of the outer neuronal membrane layer, ten times more than in non-neuronal cells. Membrane gangliosides accumulate mainly in small dynamic membrane compartments called *lipid rafts*, characterized by high concentrations of glycosphingolipids and cholesterol (48).

Ganglioside biosynthesis takes place in the Golgi complex in parallel pathways, with the addition of neutral sugar and sialic acid moieties to a glucosylceramide molecule, catalysed by specific glycosyltransferases. Once synthesized, gangliosides are transferred to the outer leaflet of the neuronal membranes, through the trans-Golgi network, where they fulfill many different physiological tasks (mainly modulation of ion channels and transporters, Ca^{2+} homeostasis regulation, neuronal development, synaptic transmission modulation), but also can be a target of anti-ganglioside auto-antibodies during GBS (48).

1.10 Anti-ganglioside antibodies action at the NMJ: role of the complement system

Patients affected by different GBS subtypes display different anti-ganglioside antibodies (AGAbs) in their sera, that at least in part explain the clinical differences amongst GBS cases. Remarkably, MFS is very strongly associated (>90% of cases) with complement binding IgG antibodies against GQ1b (anti-GQ1b antibodies) (49). Up to 50% of MFS sera also display reactivity toward other gangliosides such as GT1a, GD3, GD1b and occasionally GT1b (50). Moreover, different nervous system structures can express different ganglioside patterns and levels. For example, extraocular cranial nerves display high levels of immunoreactive MFS-related gangliosides. Noteworthy, NMJs at extraocular muscles (EOMs), the six muscles that control the movements of the eyes, were shown to be enriched of GQ1b, GT1a and GD1b gangliosides (51).

This data might explain the ophthalmoplegia characterizing MFS and, together with other considerations, makes NMJ a possible target of MFS: i) NMJ lies outside the blood-nerve barrier (BNB) (13), making it easily accessible to circulating antibodies; ii) the MAT is gangliosides-rich; iii) GBS/MFS symptoms overlap with those of known NMJ disorders, such as botulism and myasthenia gravis (48). Moreover, anti-GQ1b IgGs and IgMs have been demonstrated to bind to the NMJ, and anti-GQ1b-positive MFS sera induces in *ex vivo* mouse diaphragm preparations a transient but

dramatic rise of spontaneous release from MATs (termed miniature endplate potentials, MEPPs), together with asynchronous muscle twitching, followed by permanent paralysis (21,48). These effects resemble those triggered by the presynaptic neurotoxin α-latrotoxin (α-LTX). Anti-GQ1b antibodies actions at NMJ are hence termed the '*α-latrotoxin-like effect*' (21).

It is conceivable that the electrophysiological similarities between anti-GQ1b antibodies and α-LTX imply a shared molecular mechanism of action at the NMJ. α-LTX is a pore-forming neurotoxin whose toxicity is Ca^{2+} mediated. Also anti-GQ1b antibodies action at NMJ implies the formation of a pore-forming complex upon activation of the complement system and alteration of Ca^{2+} homeostasis, and this can be extended to all GBS-related AGAbs. Indeed, the most common AGAbs detected in patients' sera are IgG1, IgG3 or IgM isotypes, i.e. those isotypes with complement-activating features.

The complement system is a complex group of 35-40 soluble proteins playing crucial roles in innate and acquired host defense mechanisms against infection, such as cytolysis, phagocytosis, and inflammation (52). Proteins of the complement system are synthesized by the liver, and circulate in the blood as inactive precursors (pro-enzymes). The complement system can be activated by three different pathways, termed the classical, the lectin and the alternative pathways. All three pathways are activated in a sequential manner, with activation of one component leading to the activation of the next. The classical pathway is dependent on those antibodies (IgG1, IgG3, IgM) present in immune-complexes capable of activating the first component of the classical pathway, namely C1 complex, through recruitment of the C1q subunit. The activation of the lectin pathway is induced by binding of the mannose binding lectin to mannose residues on the cellular surface of pathogens. The alternative pathway is triggered when the C3b protein directly binds to the pathogen surface. All the three pathways converge in the activation of C3, the central protein of the complement system. Upon activation the C3 molecule can be covalently attached to target surfaces, where it leads to either opsonization, or cytolysis by means of the lytic pathway of the complement system. The lytic pathway begins with the production of C5 convertase which cleaves C5 to C5b and C5a. The membrane inserted C5b in turn initiates the self-assembly of the final effector of the complement lytic pathway, the membrane attack complex (MAC) (also called terminal complement complex, TCC) (52).

MAC is a supramolecular organization of molecules assembled at the target membrane. It contains one copy each of C5b, C6, C7 and C8, together with 12-18 copies of C9, the latters inserted into the target membrane, forming a cylinder-shaped pore-forming complex. The inner diameter of the

MAC pore is 110 Å, the outer diameter 220 Å, and the height of the MAC "cylinder" is 90 Å (53,54) (Fig. 2).

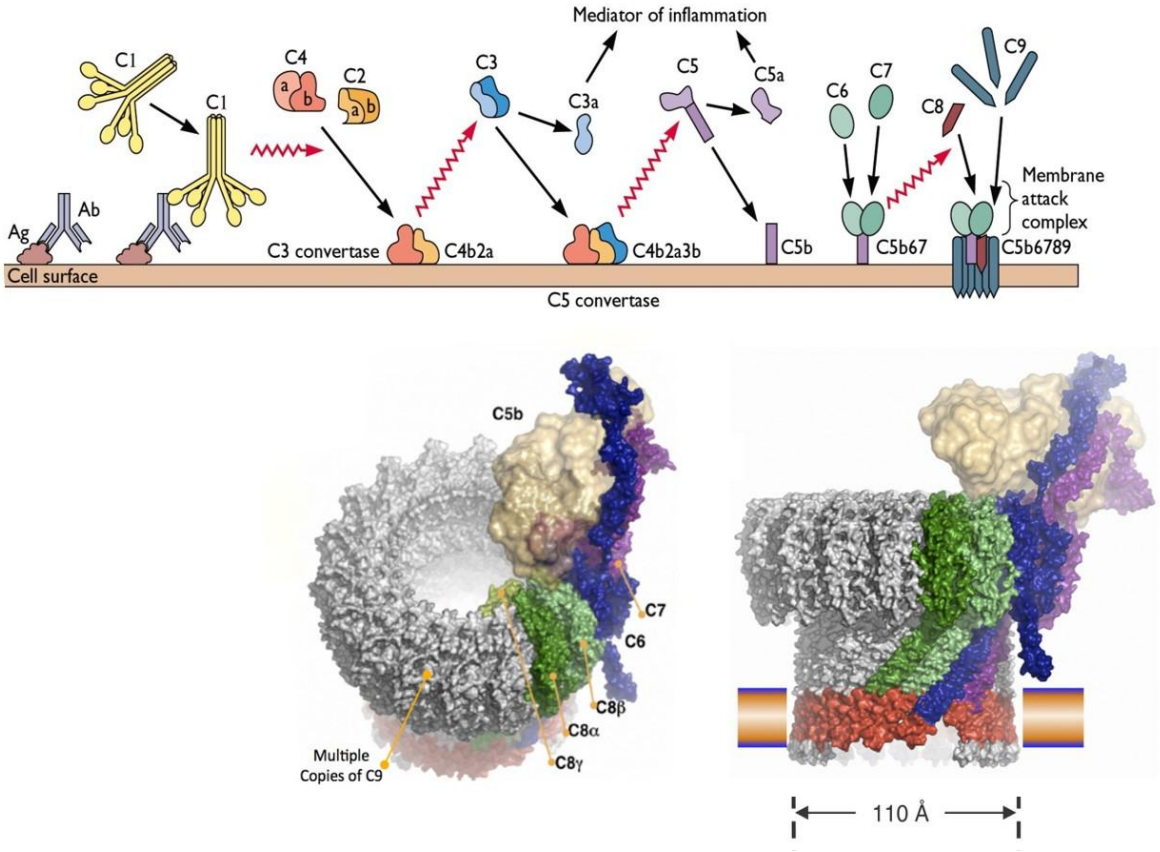

Figure 2: **The classical pathway of the complement system.** Plasma membrane antigen-bound antibodies (IgM or IgG) are able to trigger activation of the classical complement system through recruitment of C1q complex. The following cascade of proteolytic events activates other complement proteins and eventually the deposition of the membrane attack complex (MAC) at the target membrane occurs. In the images below, two views of a three-dimensional atomic model for the mature MAC, viewed from different directions, are depicted (adapted from *Aleshin et al, 2012, Journal of Biological Chemistry*).

Nowadays, overwhelming evidence supports the key role of complement in GBS. In particular, anti-GQ1b antibodies action at MAT has been deeply studied by Prof. Willison's laboratory in *ex vivo* murine nerve-muscle preparations, employing MFS sera, as well as anti-GQ1b antibodies in combination with a source of complement system proteins, i.e. normal human serum (NHS). The use of NHS is necessary because endogenous mouse complement fails to generate pathological lesions in AGAbs models, possibly due to protective mechanisms at NMJ and/or lack of activity of one of the murine complement component (55).

Immunohistochemical analysis of paralyzed muscles revealed deposits of complement products, including MAC, at NMJ, as well as anti-GQ1b antibodies (21,56). MAC deposition at NMJ led to MAT breakdown, which appears swollen and electron-lucent, with presence of abnormalities clearly indicating advanced MAT degeneration: cytoskeletal degradation and disorganization, synaptic vesicles depletion, damaged mitochondria and reduced contact with the postsynaptic MF (36). The causal relationship between complement cascade activation and MAT damage exerted by anti-GQ1b antibodies was conclusively established by employment of C6 or C7- depleted sera (56) or complement inhibitors (57), which prevented MAT degeneration.

The abovementioned alterations at MAT are akin to those observed with α-LTX, which are Ca^{2+} dependent. Also MAC effects are dependent on Ca^{2+}- and Ca^{2+}-activated proteases, as calpain inhibitors were protective for MAT (58). In other words, in MFS murine models MAC is the α-LTX-like protein complex which localizes at the MAT and induces a Ca^{2+} dependent insult, morphologically and electrophysiologically similar to that caused by α-LTX (Fig. 3).

Even though some AGAbs can also act in a complement-independent way at the NMJ (59), this has not been observed for anti-GQ1b antibodies, and MAC formation is considered the major toxic stimulus at NMJ.

In summary, AGAbs *plus* complement represents the intrinsic pathogenic stimulus responsible for MAT degeneration, with anti-GQ1b antibodies being the trigger and the complement system the effector of this dual system.

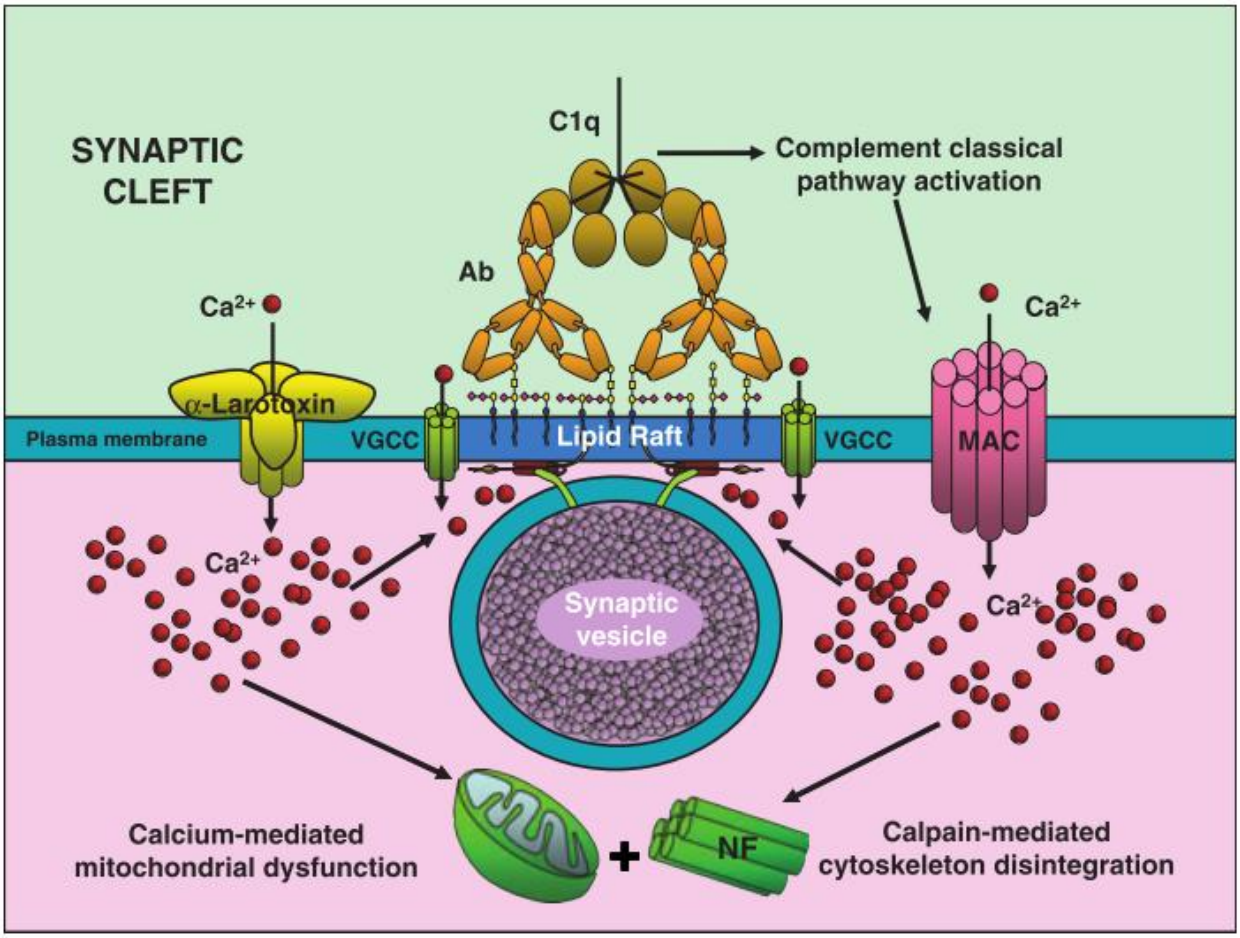

Figure 3: The effects of α-LTX and MAC at the NMJ. Schematic diagram depicting the events occurring at MAT exposed to α-LTX or anti-ganglioside antibodies in presence of complement. Upon deposition of the pore the large entry of Ca^{2+} inside the terminal induce a massive synaptic vesicles exocytosis and calcium/calpain mediated intra-terminal injury, including cytoskeletal degradation and mitochondrial injury (*Willison, 2007, Journal of Neurochemistry*).

2. AIM

The general purpose of this PhD project is to provide a better understanding of the complex inter- and intracellular signalling that govern MAT degeneration and regeneration.

To achieve this aim, I have set-up novel *in vivo* and *in vitro* models of Miller Fisher syndrome, based on the combination of FS3, a monoclonal anti-GQ1b/GT1a antibody (kindly provided by Prof. Nobuhiro Yuki, Department of Neurology, Mishima Hospital, Niigata, Japan) with normal human serum (NHS) as a source of the complement proteins. The FS3+NHS complex represents the "*pathogen*" responsible for the reversible acute injury of MATs of this peripheral autoimmune neuropathy.

Once established, this model has been employed to identify alarm molecules (*alarmins*) released after MAT injury and involved in PSCs activation, as well as to study the intracellular pathways involved in PSCs pro-regenerative phenotypic shift.

3. MATERIALS & METHODS

3.1 Reagents

The mouse monoclonal antibody (FS3, isotype IgG2b-κ) was previously characterized (46). For immunization mice were inoculated with a heat-killed *C. jejuni* lysate, the infectious agent frequently associated with MFS. FS3 recognizes gangliosides GQ1b and GT1a, the latter being identical to GQ1b except for one sialic acid residue less. Normal human serum (NHS) from a pool of human healthy males AB plasma (Sigma-Aldrich #H4522, lot #SLBG2952V) was employed as a source of complement. Unless otherwise stated, all reagents were purchased from Sigma.

3.2 Primary cell cultures and co-cultures

Rat primary cultures of cerebellar granular neurons (CGNs), spinal cord motor neurons (SCMNs), primary Schwann cells (SCs) and their relative co-cultures were prepared as described previously (18,60,61).

3.3 Mice

Experiments were performed in Swiss-Webster adult CD1 mice or C57BL/6 mice expressing cytosolic GFP under the *plp* promoter via the collaboration of Thomas Misgeld (Munchen, Germany). All procedures were performed in accordance with the Council Directive n° 2010/63/EU of the European Parliament and approved by the Italian Ministry of Health.

3.4 NMJ immunohistochemistry

For binding studies whole *Levator auris longus* (LAL) and EOMs were incubated *ex-vivo* with FS3 10 µg/mL at 10°C for 15-30 min, then washed, fixed and processed for immunofluorescence (see below). In the studies of FS3 internalization at MAT, some muscles were additionally incubated at 37°C for 30 minutes.

For MAC deposition analysis FS3 (10 µg) was diluted with NHS 50% (v/v) in 100 µL of physiological saline (0.9% wt/v NaCl in distilled water), and injected s.c. in proximity of LAL muscle of anesthetized CD1 of around 20–25 g; muscles were collected after 2 h. In the case of EOMs, an *ex vivo* incubation was performed (FS3 10 µg/mL + NHS 50% v/v, 1 h at 37°C). Heat inactivation of NHS (56°C for 30 min, HI-NHS), or treatment with NHS 50% alone were employed as negative controls.

To define the kinetics of nerve terminal degeneration and regeneration in mice, FS3 (10 µg) was diluted with NHS 50% (v/v) in 100 µl physiological solution, and subcutaneously injected close to LAL muscles, or intramuscularly in the mice hind limb for different time points.

Muscles were then fixed in 4% (wt/vol) PFA in PBS for 15 min at room temperature, quenched in PBS + 50 mM NH_4Cl, and then permeabilized and saturated in blocking solution: 15% (v/v) goat serum, 2% (wt/v) BSA, 0.25% gelatin, 0.20% (wt/v) glycine, and 0.5% Triton X-100 in PBS 2 h at room temperature. Incubation with the following primary antibodies was carried out for 48-72 h in blocking solution: anti-neurofilaments 200 (mouse monoclonal, anti-NF, 1:200, # N5389), anti-VAchT (rabbit polyclonal, 1:1000, Synaptic Systems), anti-C5b-9 (rabbit polyclonal, 1:1000, Abcam, #ab55811). Muscles were then washed and incubated with secondary antibodies (Alexa-conjugated, 1:200, Life Technologies). Nuclei were stained with Hoechst. NMJs were identified by Alexa-conjugated α-bungarotoxin (α-BTx, 1:500, Life Technologies, #B35451). Images were collected with a Leica SP5 confocal microscope equipped with a 63× HCX PL APO NA 1.4.

3.5 Electrophysiological recordings

Mice were sacrificed at scheduled times by anaesthetic overdose followed by cervical dislocation, soleus muscles dissected and subjected to electrophysiological measurements. Three mice were

used for each condition at each time point. Electrophysiological recordings were performed in oxygenated Krebs-Ringer solution on sham or FS3+NHS injected soleus muscles using intracellular glass microelectrodes (WPI, Germany) filled with one part of 3M KCl and two parts of 3M CH_3COOK.

Evoked neurotransmitter release was recorded in current-clamp mode, and resting membrane potential was adjusted with current injection to −70mV. Evoked junction potentials (EJPs) were elicited by supramaximal nerve stimulation at 0.5 Hz using a suction microelectrode connected to a S88 stimulator (Grass, USA). To prevent muscle contraction, samples were incubated for 10 min with 1 μM μ-Conotoxin GIIIB (Alomone, Israel). Signals were amplified with intracellular bridge mode amplifier (BA-01X, NPI, Germany), sampled using a digital interface (NI PCI-6221, National Instruments, USA) and recorded by means of electrophysiological software (WinEDR, Strathclyde University). EJPs measurements were carried out with Clampfit software (Molecular Devices, USA), statistical analysis with Prism (GraphPad Software, USA).

3.6 Calcium imaging

Primary neurons or their co-cultures with SCs were loaded for 10 min with the calcium indicator Fluo-4 AM (4 μM, Life Technologies, #F14201), washed and transferred to the stage of an inverted fluorescence microscope (Eclipse-Ti; Nikon Instruments), equipped with the perfect focus system (PFS; Nikon Instruments) and with high numerical aperture oil immersion objectives (60X). Calcium signals were recorded in control samples and in samples exposed to FS3 0.1 μg/mL + NHS 0.5 % (v/v), or NHS, or FS3+HI-NHS, with excitation of the fluorophore performed at 465-495 nm by means of an Hg arc lamp (100 W; Nikon). Emitted fluorescence was collected at 515-555 nm. Fluorescence (F) was measured in a selected region of interest (ROI) containing cell cytosol and corrected for background. Measurements were expressed as F/F0 fold increase (%), where F0 represents the fluorescence level at t=0. Images were acquired every 20 sec. In some experiments apyrase (1.5 U/ml) was added 15 min before image acquisition and left throughout.

3.7 Immunofluorescence

For binding experiments CGNs (6 DIV, *days in culture*) or SCMNs (4-5 DIV), plated onto 35-mm dishes or 24 well-plates, were exposed to FS3 0.1 μg/mL at 16°C for 20 min in Krebs Ringer buffer for CGNs (KRH: Hepes 25 mM at pH 7.4, NaCl 124 mM, KCl 5 mM, $MgSO_4$ 1.25 mM, $CaCl_2$ 1.25 mM, KH_2PO_4 1.25 mM, glucose 8 mM), and in E4 medium for SCMNs (E4: 120 mM NaCl, 3 mM KCl, 2 mM $MgCl_2$, 2 mM $CaCl_2$, 10 mM glucose, and 10 mM Hepes, pH 7.4). Cells then washed, and subjected to immunofluorescence (see below).

For studies on MAC deposition and *bulge* characterization neurons were exposed to FS3 0.1 μg/mL + NHS 0.5 % (v/v) at 37°C for 20 min.

Following treatments cells were washed, fixed for 10 min in 4% (wt/v) paraformaldehyde (PFA) in PBS and quenched (0.38% glycine, 50 mM NH_4Cl in PBS) at room temperature. Cells were permeabilized and saturated in buffer A (20 mM PIPES, 137 mM NaCl, 2.7 mM KCl, pH 6.8) containing 5% (v/v) goat serum, 50 mM NH_4Cl and 0.5% (wt/v) saponin for 45 min. Slices were incubated overnight in buffer A *plus* 5% goat serum and 0.1% (wt/v) saponin with the following primary antibodies: anti-C5b-9 (rabbit polyclonal, 1:5000, Abcam), VAMP2 (1:500, Rossetto et al., 1996).

For immunofluorescence in neurons-SCs co-cultures, samples were fixed and quenched as above, and permeabilized with 0.3% Triton X-100 in PBS for 5 min at room temperature (RT). After saturation with 3% (v/v) goat serum in PBS for 1 h, they were incubated with primary antibodies (anti-phospho-p44/42 MAPK (1:500, Cell Signaling, #9101); anti-phospho-CREB, 1:500, Cell Signaling, #9198S); anti-S100 (1:200, #S2532)) diluted in goat serum 3% (v/v) in PBS overnight at 4°C.

After washes, samples were incubated with the correspondent secondary antibodies (Alexa-conjugated, 1:200; Life Technologies). Nuclei were stained with Hoechst. Coverslips were mounted in ProLong Diamond (Thermo Fisher) and examined by epifluorescence (Leica CTR6000) microscopy.

3.8 Mitochondrial imaging

SCMNs or CGNs were loaded with tetramethylrhodamine methyl ester (TMRM, Life Technologies) 10 nM for 10 min at 37°C, washed and equilibrated at room temperature for 10 min before FS3+NHS addition (FS3 0.1 μg/mL + NHS 0.5 % (v/v) for 10 min). At the end of each experiment 10 μM carbonyl cyanide-p-trifluoromethoxyphenylhydrazone (FCCP), a known mitochondrial electron chain uncoupler, was added as positive control. For mitochondrial morphology studies cells were loaded with Mitotracker Red (Life Technologies) 25 nM for 10 min at 37°C and then washed prior to image acquisition.

3.9 Hydrogen peroxide detection

Hydrogen peroxide was measured in primary neurons exposed to FS3 0.1 μg/mL + NHS 0.5 % (v/v) for 20 min using Mitochondria Peroxy Yellow 1 (MitoPY1) or Peroxyfluor 6 acetoxymethyl ester (PF6-AM), probes specific for mitochondrial and cytoplasmic H_2O_2 detection, respectively (29,62). Both probes were loaded at 5 μM for 30 min at 37 °C in E4 medium (SCMNs) or KRH (CGNs).

3.10 Western blotting

SCMNs+SCs co-cultures were exposed to FS3 0.1 μg/mL + NHS 0.5 % (v/v). In some samples cells were preincubated with catalase (500 U/well, #C1345, 5' preincubation) or apyrase (1.5 U/ml, #A7646, 15' preincubation) before intoxication and left throughout.

For internalization studies, SCMNs or CGNs were incubated with FS3 2 μg/mL for different time periods.

Following treatments samples were lysed in lysis buffer (4% SDS, 0.125 M Tris-HCl, protease inhibitors Cocktail-Roche-, #04 693 132 001, and phosphatase inhibitor cocktail, #P0044). Total lysates were loaded on Precast 4–12% SDS-polyacrylamide gels (Life Technologies) and transferred onto nitrocellulose paper in a refrigerated chamber.

After saturation, membranes were incubated overnight with rabbit polyclonal antibodies (anti-phospho-p44/42 MAPK (1:1000, Cell Signaling, #9101); anti-phospho-CREB, 1:1000, Cell Signaling,

#9198S)) followed by an anti-rabbit secondary antibody HRP-conjugated (Life Technologies, 1:2000). Chemiluminescence was developed with the Luminata TM Crescendo (Millipore), and emission measured with ChemiDoc XRS (Bio-Rad). For densitometric quantification, the bands of interest were normalized to the housekeeping protein Hsp90 (mouse monoclonal, 1:1000, BD Transduction Laboratories, #610419). Band intensities were quantified on the original files with the software Quantity One (Bio-Rad). None of the bands reached saturation.

3.11 ATP measurements

ATP was quantified in the supernatants of primary neurons using the commercial ATP Lite One-Step kit (Perkin-Elmer, #6016941), which relies on a luminescence-based ATP-dependent reaction. Cells were exposed for different time periods to FS3 (0.1 μg/mL) in combination with NHS (0.5% v/v), as well as to appropriate control conditions. Ecto-ATPases and NHS-ATPases activities were quenched by the addition of 1 mM sodium orthovanadate in the incubation medium. For each well the ATP released was estimated as the ratio between ATP in the supernatant and total cellular ATP (cell lysis by Triton X-100 0.5% v/v), and expressed as percentage of the untreated control. Quick centrifugation of supernatants was performed to eliminate cell debris before measurements. Luminescence was measured with a luminometer (Infinite M200 PRO, Tecan).

3.12 Lactate dehydrogenase activity assay

CGNs plated on 24-well plates (250,000 cells/well) were exposed to saline, NHS, FS3 (0.1 μg/mL) + NHS (0.5% v/v), or FS3 + HI-NHS for 30 min. Supernatants were collected and lactate dehydrogenase (LDH) activity was measured following manufacturer's instructions (Sigma, #TOX7) and normalized by total cellular LDH activity from cell lysates. Each sample was expressed as percentage of the positive control (cell lysates by Triton X-100 0.5%).

3.13 Cyclic AMP detection

Epac-S^{H187}, a fourth generation of *Epac-based* FRET probe for cAMP detection was employed. This sensor consists of the cAMP-binding protein EPAC sandwiched between mTurquoise2, a very bright and bleaching resistant donor fluorescent protein, and a novel acceptor cassette consisting of a tandem of two Venus fluorophores (63). Briefly, SCs co-cultured with neurons were transfected with 1 μg of the probe with Lipofectamine 2000 (Life Technologies, #11668-027). Experiments were performed 24 hours after transfection. Cells were monitored using an inverted fluorescence microscope (Eclipse-Ti; Nikon Instruments) equipped with the perfect focus system (PFS; Nikon Instruments). Excitation of the fluorophore was performed by an Hg arc lamp (100 W; Nikon) using a 435-nm filter (10-nm bandwidth). YFP and CFP intensities were recorded with a cooled CCD camera (C9100-13; Hamamatsu) equipped with a 515-nm dichroic mirror at 530 nm (25-nm bandwidth) and 470 nm (20-nm bandwidth) respectively. Signals were digitized and FRET was expressed as the ratio between donor (CFP) and acceptor (YFP) signals (CFP/YFP). YFP and CFP intensities were corrected for background. Co-cultures were pre-incubated with 1 mM sodium orthovanadate as general ATPase inhibitor for 5 min, then, after 1 min recording, cells were exposed to FS3 (0.1 μg/mL) + NHS (0.5% v/v), or NHS, or FS3 + HI-NHS. A final stimulation with 25 μM forskolin was performed at the end of each experiment to maximally raise cAMP levels.

4. RESULTS

4.1 Set-up of a novel *in vivo* model of MFS

To date, most of the animal models of MFS based on anti-GQ1b antibodies *plus* complement were *ex vivo* muscle preparations, and were mainly employed to study the acute effects of anti-GQ1b antibodies *plus* complement, i.e. the early pathogenic steps of MAT degeneration, leaving the processes leading to MAT regeneration unexplored (21,36,56,58,64).

More recently, Rupp and colleagues reported the first *in vivo* model of MFS, where MAT degeneration and regeneration kinetics were followed after topical application of a monoclonal anti-GQ1b IgG antibody *plus* NHS (65). Briefly, after midline excision of anesthetized and intubated mice, sternohyoid and sternomastoid muscles were exposed to anti-GQ1b antibody (120 µg per mouse) for 30 minutes and soon after to NHS (40% v/v, diluted in a total volume of 0.6 mL) for additional 30 minutes. Hence, skin suture in the ventral neck area was performed and mice were sacrificed after different days post-surgery, and NMJs of treated muscles processed for immunohistochemistry analysis. By this approach the totality of NMJs recovered completely in 5 days post-injury (65).

Although of great value, the work of Rupp and colleagues is mostly phenomenological, and the molecular players involved in MAT regeneration were not studied. In addition, although such surgical procedure allows to expose the muscles to a large quantity of antibody and NHS (see above), it displays a certain degree of invasiveness, that could negatively influence or mask the identification of those molecular signals and cellular pathways involved in cell-to-cell communication.

Taking in account these considerations, the establishment of a novel model of MFS was crucial for a molecular study of the intercellular and intracellular signalling events underlying MAT degeneration and regeneration observed in MFS. We therefore set-up a murine model of MFS based on the combination of the complement-fixing (isotype IgG2b-κ) anti-GQ1b/GT1a monoclonal antibody FS3 (kindly provided by Prof. Nobuhiro Yuki, Department of Neurology, Mishima Hospital, Niigata, Japan), and NHS as a source of complement. This novel model provides the advantage of minimal surgical procedures (needle injection) and reduced volume of injection (see below), due to strong affinity of FS3 to neuronal membranes, with important reduction of

inflammatory response upon FS3 *plus* complement injection. Consequently, this model is suitable for molecular studies, as controllable and minimally invasive.

4.1.1 Anti-GQ1b antibody binds to and is internalized by motor axon terminals.

As a first step, we characterized the binding properties of FS3 at different murine muscles: the *Levator Auris Longus* (LAL) muscle and extra-ocular muscles (EOMs). LAL muscle belongs to mouse cranial muscles and, because of its flatness, is ideal for imaging studies (18,66). EOMs are the muscles firstly affected in MFS, the specific targets of anti-GQ1b autoantibodies, and highly enriched in GQ1b and GT1a gangliosides (49,51).

We performed immunohistochemical analyzes in LAL and EOMs nerve-muscle preparations incubated *ex vivo* with FS3 at 10°C, in order to slow down endocytic processes, and we observed that FS3 avidly binds to NMJs, and co-localizes with the presynaptic vesicular acetylcholine transporter (VAchT) (Fig. 4A).

We also performed *ex vivo* binding of FS3 at LAL and EOMs followed by incubation of the muscles at 37°C for 30 minutes. This procedure caused the loss of FS3 selective plasma membrane localization (Fig. 4B), indicating FS3 internalization inside the MAT. Orthogonal projections from confocal images confirmed that FS3 staining is indeed inside the terminal (Fig. 4C). These results are in line with recent works of Prof. Willison's group, which demonstrate that AGAbs are endocytosed by MAT, and consequently removed from the blood circulation, which represents a protective mechanism which attenuates complement-mediated cytotoxicity (67,68).

We analysed also *in vitro* FS3 internalization in cultured neurons: we incubated the antibody with spinal cord motor neurons (SCMNs) and cerebellar granular neurons (CGNs) for different time periods. Hence cells were lysed in non-denaturing conditions, protein lysates separated by electrophoresis, and FS3 content in each sample assessed with an anti-mouse-HRP. Western blot experiments indicate that FS3 progressively accumulates inside neurons (Fig. 4D), in line with *in vivo* results.

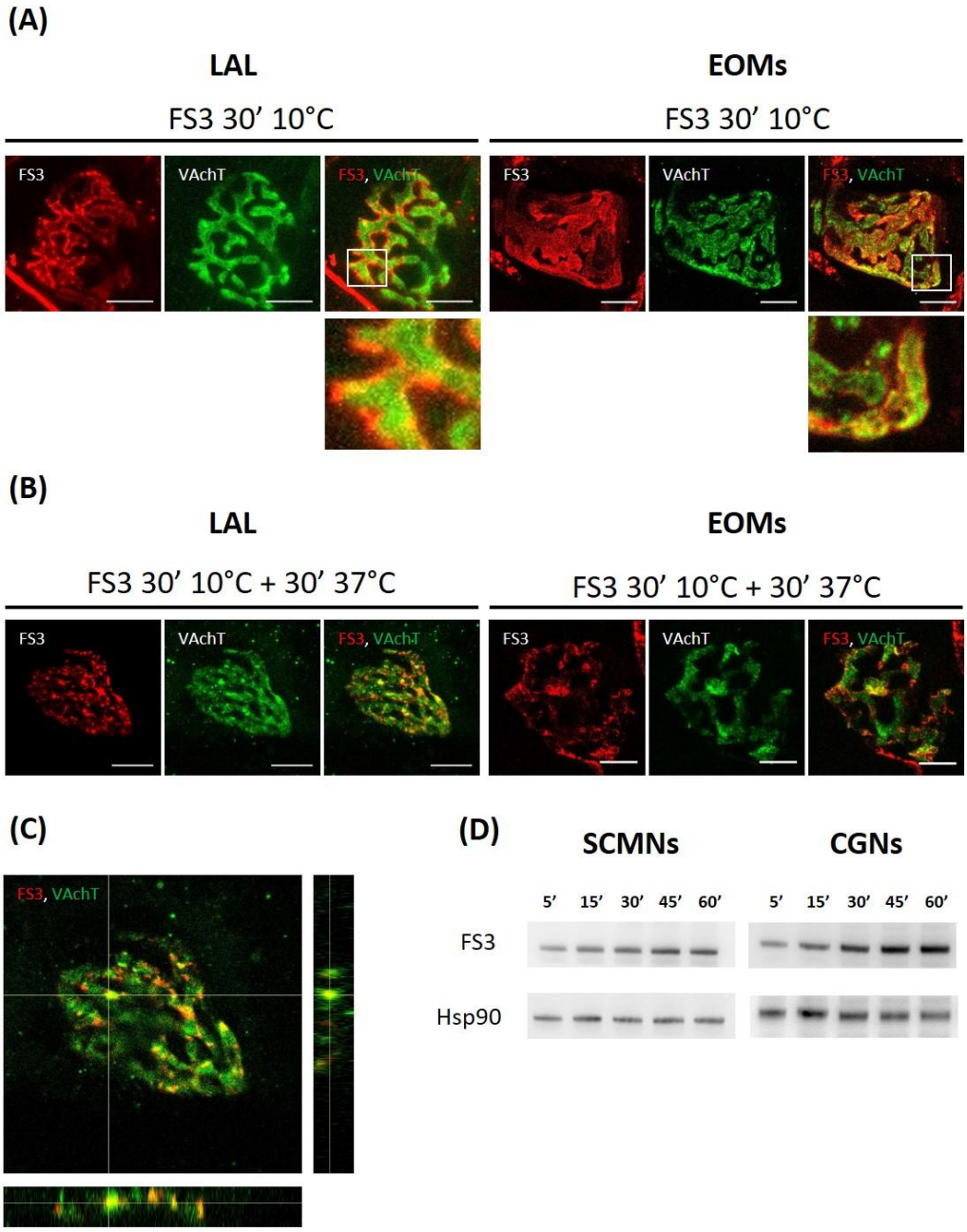

Figure 4: FS3 internalization in vivo and in vitro. (A) Muscle-nerve preparations of LAL muscles (left panels) and EOMs (right panels) were incubated with FS3 at 10°C and subjected to immuno-histochemical analysis. FS3 (*red*) binds to presynaptic nerve terminals that are stained by an anti-VAchT antibody (*green*). (B) FS3 is internalized upon 30 minutes incubation at 37°C. (C) Orthogonal projection of confocal images showing FS3 staining inside motor axon terminals. Scale bars: 10 μm. (D) Spinal cord motor neurons (SCMNs) or cerebellar granular neurons (CGNs) were exposed to FS3 for different time points and lysed in non-denaturing conditions. Western blot analysis shows FS3 progressive accumulation inside neurons. One representative Western blot out of 3 experiments is shown. Hsp90 is used here as internal standard.

4.1.2 Anti-GQ1b antibody triggers complement activation at EOMs motor axon terminals

EOMs are main targets of anti-GQ1b antibodies in MFS (49). Indeed, ophthalmoplegia belongs to the triad of symptoms hallmarking this disease (40). We therefore studied the effects of a combination of FS3 with a source of complement proteins (normal human serum, NHS) at MATs of *ex vivo* preparations of EOMs. FS3, when combined to NHS (FS3+NHS) for 1 h at 37°C, triggers the formation and deposition of the final effector of the complement system, the membrane attack complex (MAC), as detected by a specific antibody for C5b-9 complex (Fig. 5, upper panel). This leads to the disappearance of the staining of neurofilaments (NFs) at MAT, due to nerve terminal degeneration.

MAT degeneration is FS3- and complement- dependent, as heat inactivation of complement proteins of the NHS (56°C for 30 min, HI-NHS) or incubation with NHS 50% alone prevents MAC deposition and neurodegeneration (Fig. 5, middle and lower panels).

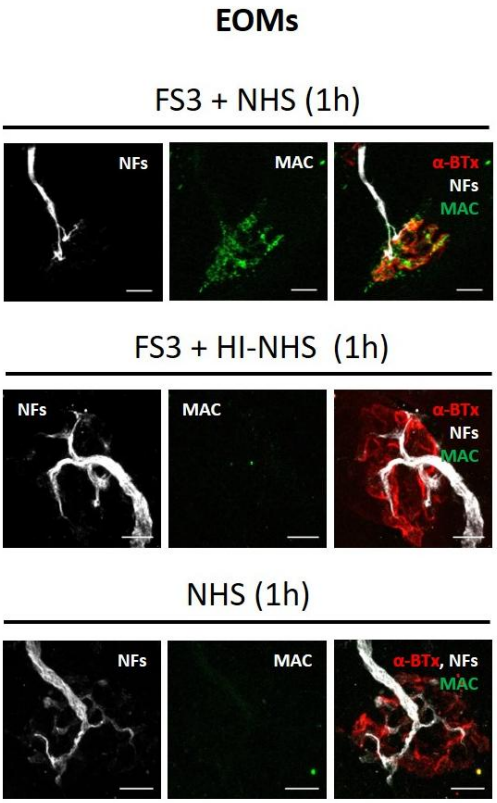

Figure 5: FS3 binding to GQ1b/GT1a gangliosides triggers MAC deposition in the presence of complement and nerve terminal degeneration in EOMs. FS3+NHS leads to MAC deposition (*green*) on neuronal surface of *ex-vivo* treated EOMs (1 hour incubation). The presynaptic element is identified by NF staining (*white*), the postsynaptic one by fluorescent α-BTx (*red*). MAC-triggered neurodegeneration is complement- and FS3- dependent, as no nerve terminal fragmentation is detectable in FS3+HI-NHS or NHS treated NMJs (middle and lower panels). Scale bars: 10 µm.

4.1.3 Anti-GQ1b antibody *plus* complement triggers a reversible neurodegeneration of motor axon terminals *in vivo*

EOMs represent a useful tool to study anti-GQ1b antibodies- mediated damage at MAT. However, due to accessibility costraints they are not suitable for *in vivo* experiments (the skull, which tightly closes and protects the eye, prevents to perform local injections at EOMs). We therefore moved to other muscles to be able to follow entirely the kinetics of FS3+NHS- induced nerve terminal degeneration, as well as the subsequent nerve terminal regeneration.

With these purposes, we administered FS3 (10 µg per mouse) *plus* NHS (50% v/v) subcutaneously in LAL muscles of living CD1 mice for different time periods, and looked at NMJ morphology by immune-histochemical analysis. Noteworthy each mouse received a single acute injection of antibody *plus* complement in a small volume (100 µL) of physiological saline, in the absence of surgery, with very limited invasiveness. By this approach, we observed MAC deposition at MATs within 2h after FS3+NHS administration (Fig. 6A), followed by a progressive degeneration of MATs, monitored by the disappearance of NFs and VAchT stainings over time (Fig. 6B, left panel). Maximum degeneration occurred after 24h treatments, with 61% NMJs lacking both NFs and VAchT stainings (144 NMJs analyzed, 3 independent experiments). Strikingly, 3 days post-injection MATs regrew completely, in line with the known reversibility of MFS.

Similarly to EOMs, the neurotoxic effect on LAL muscles is FS3- and complement- dependent, as neurodegeneration does not take place upon incubation with HI-NHS or in the absence of FS3 (Fig. 6B, right panel).

To obtain a quantitative estimation of FS3+NHS- induced neurodegeneration, we performed electrophysiological recordings on soleus muscles after an intramuscular injection of FS3 (10 µg) *plus* NHS (50% v/v) (total volume 100 µL) in the hind limbs for different times. Briefly, tibial nerve - soleus muscle preparations were dissected, and evoked junction potentials (EJPs) at the postsynaptic membrane of muscle fibers were elicited by supramaximal nerve stimulation and recorded. Noteworthy, EJPs are strictly dependent on a functional MAT. We found that neurotransmission is compromised at 48 hours, and is progressively restored within 9 days (Fig. 7A). This kinetics was further confirmed by immunohistochemistry, with a peak of MAT degeneration at 48h after injection (92% of degenerated NMJs, 137 NMJs analyzed, 3 independent experiments), and recovered morphology of the totality of NMJs within 9 days (Fig. 7B).

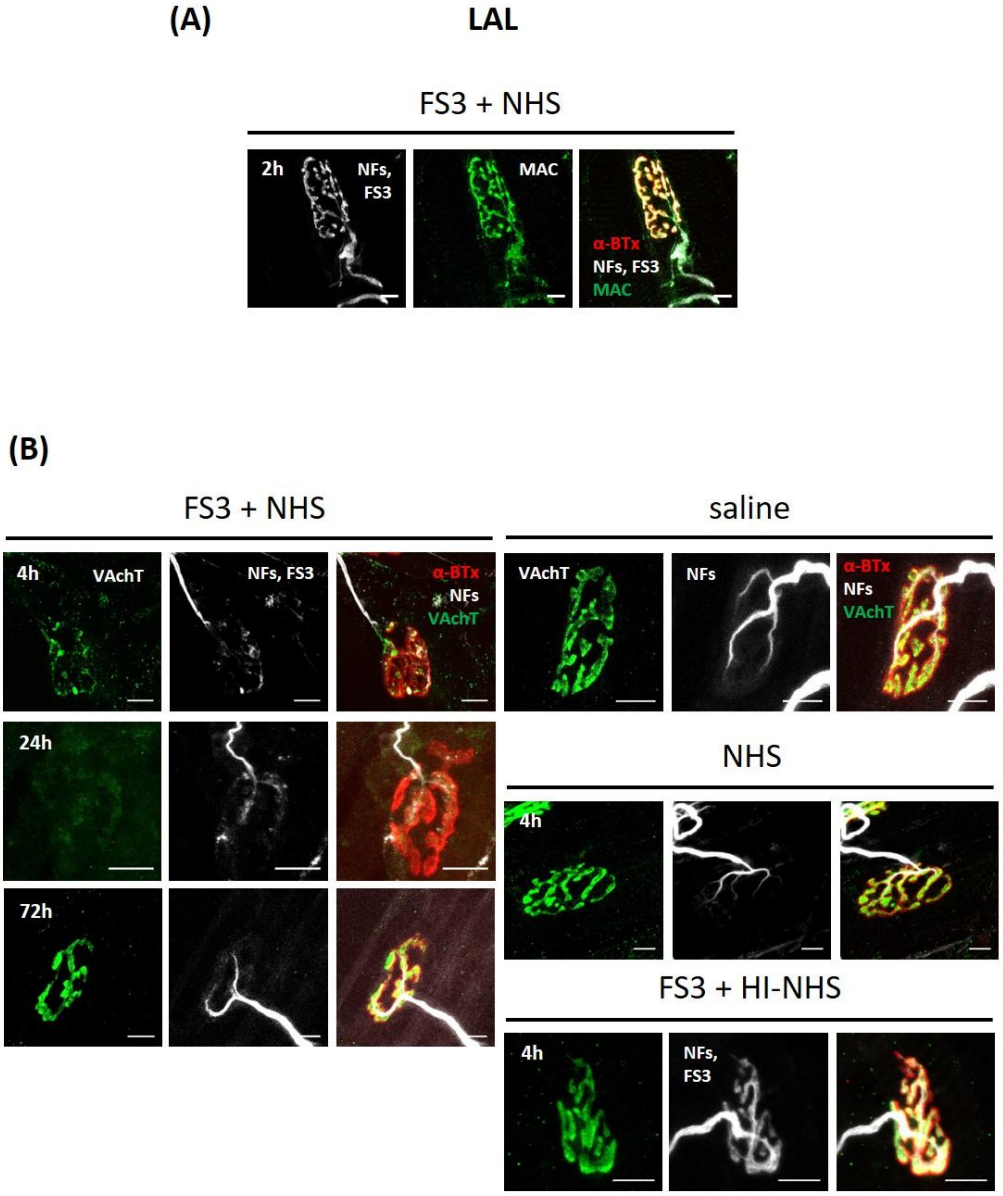

Figure 6: Anti-GQ1b plus complement triggers a reversible motor axon terminal degeneration in vivo at LAL NMJs. (A) FS3+NHS injected close to LAL muscle leads to MAC deposition (*green*) on neuronal surface. The postsynaptic element is stained by fluorescent α-BTx (*red*), while the presynaptic elements is identified by NFs and MAT-bound FS3 (*white*). (B) Kinetics of VAchT and NFs loss (*green* and *white* respectively) in LAL NMJs following injection of FS3+NHS, and subsequent recovery (left panels). Neurodegeneration depends on FS3 binding and on active complement, as no degeneration takes place upon local injection of saline, NHS or HI-NHS (right panels). Scale bars: 10 µm.

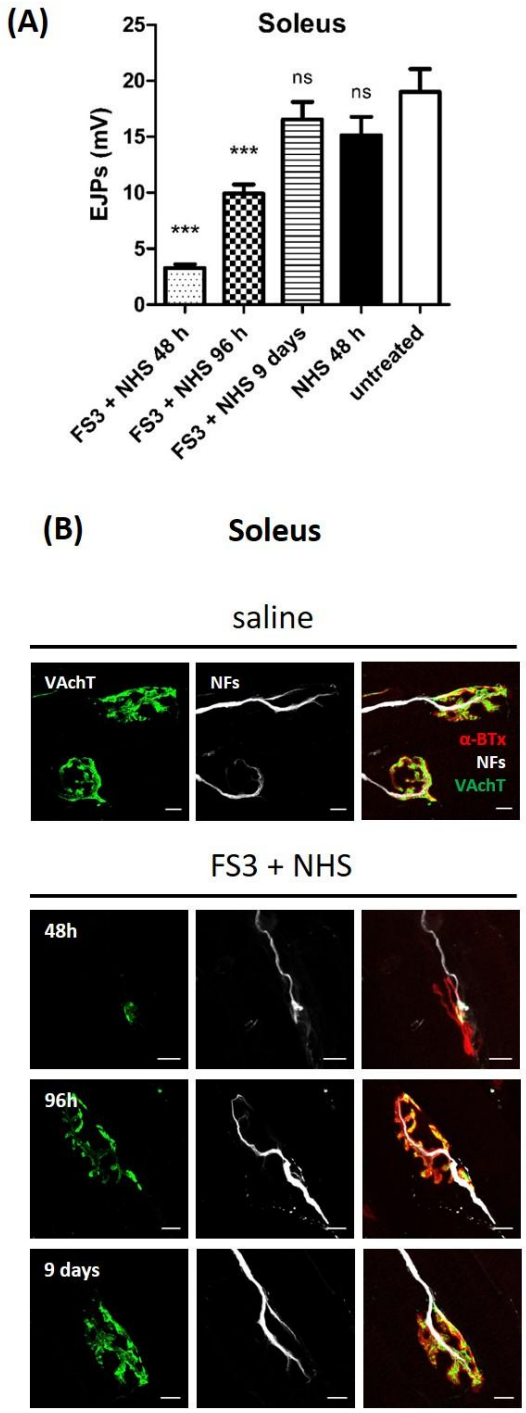

Figure 7: Anti-GQ1b plus complement triggers a reversible motor axon terminal degeneration in vivo at soleus NMJs. (A) Evoked junctional potentials (EJPs) were recorded in soleus muscles upon local injection of FS3+NHS, NHS or saline for the indicated time points. Bars represent the average EJP amplitude of 45 muscle fibres from 3 different mice/time point. Student's unpaired *t*-test, two-sides, ***$p<0.0001$ versus control (vehicle). Error bars represent SEM, ns= not significant. (B) Kinetics of VAchT and NF loss (*green* and *white* respectively) in soleus NMJs following injection of FS3+NHS, and subsequent recovery. The postsynaptic element is stained by fluorescent α-BTx (*red*). Scale bars: 10 μm.

4.1.4 Complement resistance occurs at motor axon terminals upon MAC deposition

The injection volume employed here, i.e. 100 µL, provides the minimal and sufficient quantities of anti-GQ1b antibody and complement proteins to elicit MAT degeneration. During the set-up of the model we tested a smaller injection volume, i.e. 15 µL, which provides the same amount of FS3 (10 µg per mouse), but a different amount of NHS (50% v/v). This combination resulted in an extensive deposition of MAC at MATs of LAL muscle, as assessed by immunohistochemistry (Fig. 8A); however, surprisingly, neurodegeneration failed to occur, and all MATs appeared unharmed and healthy (Fig. 8B). Therefore, MAC deposited at MAT (directly proportional to the quantity of injected NHS) can elicit terminal degeneration only when it reaches a *'toxic threshold'* (100 µL injection volume). Noticeably, in both cases MAC is deposited at MATs: it is likely that complement resistance is induced also in the 100 µL condition, but are overcome by the more massive delivery of MAC at MATs.

The putative mechanisms underlying the complement resistance behavior are commented in the Discussion section.

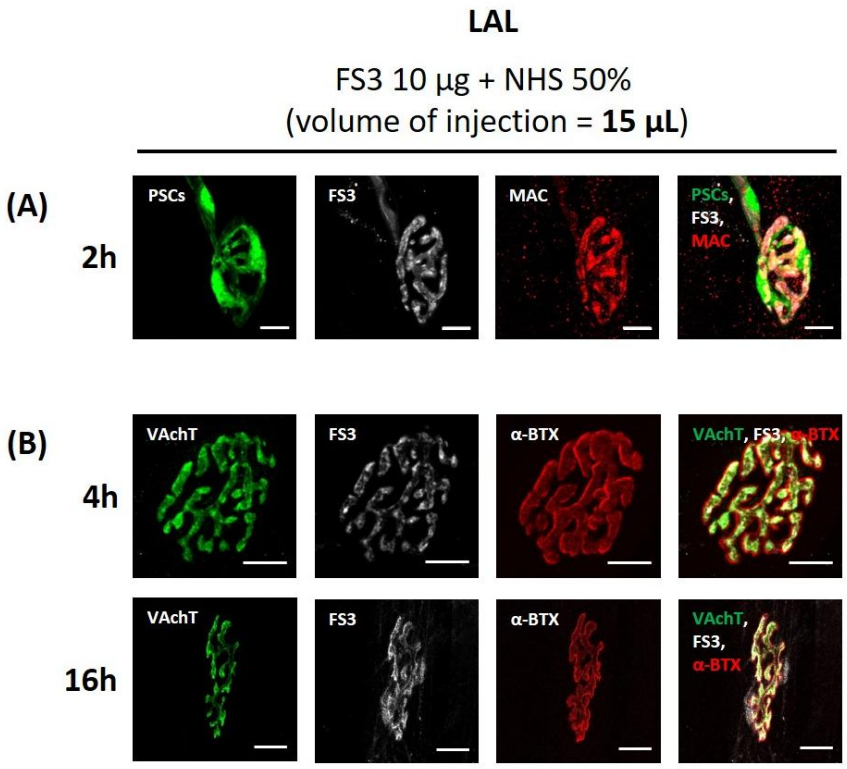

Figure 8: Nerve terminal degeneration by FS3+NHS depends on the amount of complement. (A) Injection of FS3 (10 µg) + NHS 50% v/v (15 µL total volume) leads to MAC deposition (*red*) at MAT of LAL muscles, but not to nerve terminal degeneration. NMJs are recognizable by GFP-expressing Schwann cells (*green*) and FS3 staining (*white*). (B) No MAT degeneration takes place even after longer incubation (4 and 16 h). The postsynaptic element is stained by fluorescent α-BTx (*red*). Scale bars: 10 µm.

4.1.5 Perisynaptic Schwann cells engulf debris of motor axon terminal destroyed by anti-GQ1b *plus* complement

Once established the time course of neurodegeneration following the injection of FS3 (10 µg) *plus* NHS (50% v/v) in the 100 µL total volume, we examined the morphological responses of PSCs to MAT destruction. With this purpose, we employed transgenic mice (C57BL/6 strain) expressing cytoplasmic green fluorescent protein (GFP) specifically in SCs under the *plp* promoter (69,70). Local injection of FS3+NHS in LAL muscles of these mice results in MAT degeneration that resembles that observed in CD1 mice (not shown). As soon as MAT becomes fragmented, PSCs become strongly enriched in vacuoles, likely phagosomes, containing debris from the destroyed MAT (Fig. 9). This suggests that upon anti-GQ1b *plus* complement-triggered neurodegeneration, PSCs undergo to a series of intracellular responses aimed at clearing nerve debris, a crucial step for the subsequent neuroregeneration.

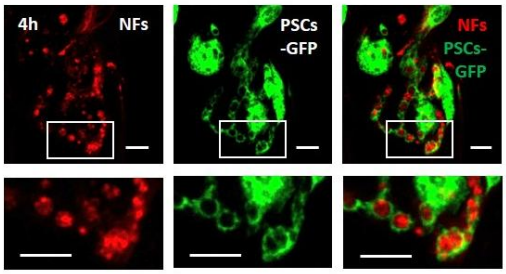

Figure 9: Phagocytosis of MAT debris by PSCs. Upon FS3+NHS injection in LAL muscles, degenerated nerve terminals stained by NF (*red*) are engulfed by PSCs (*green*). Magnification of phagosomes is shown in lower panels. Scale bars: 10 µm.

4.2 Set-up of a novel *in vitro* model of MFS

FS3+NHS mixture recapitulates in the live mouse the reversible neurodegeneration characterizing MFS. Following MAT fragmentation, we also observed a clear phagocytic response of PSCs which engulf nerve debris. To gain insights into neuron-SCs communication underpinning nerve terminal degeneration and regeneration from a molecular point of view, we performed *in vitro* experiments also in neurons-SCs primary co-cultures.

Therefore, we applied FS3+NHS also to primary neuronal cultures from the cerebellum or the spinal cord. Cerebellar granular neurons (CGNs) are an almost pure neuronal population (71), and spinal cord motor neurons (SCMNs) are the most similar to peripheral motor neurons, and are a mixed culture (72).

In *in vitro* experiments a careful assessment of FS3 and NHS concentrations is an absolute requirement, as cultured neurons are completely exposed to the stimuli, while in living animals the MAT is the only part of the motor axon not protected by the BNB. A particular attention must be paid to the amounts of NHS employed, as it contains, beside complement proteins, many different constituents and also a lot of different IgGs. It is therefore possible that some of the IgGs contained in NHS will bind to one or more antigens on the neuronal plasma membrane, thus activating the complement system also in absence of FS3. Nevertheless, a reduction of NHS concentration can prevent this aspecific MAC induction. Indeed, only six IgGs bound together to the antigen (IgGs hexamers) are efficiently able to recruit and activate C1q, the initiator of the classical complement cascade (73).

Here follows a summary of the results obtained with our novel *in vitro* model of MFS.

4.2.1 Anti-GQ1b antibody binds to primary neurons and activate complement

A prerequisite step for the *in vitro* model based on the exposure of primary neurons to FS3+NHS is the expression of GQ1b (and/or GT1a) polysialogangliosides on neuronal surface. SCMNs are primarily affected by MFS, and CGNs express GQ1b gangliosides (74,75).

Immunofluorescence revealed that, indeed, FS3 stains both CGNs and SCMNs (β_3-tubulin positive cells) (Fig. 10A). The binding is neuron-specific, as no staining was observed either in the non-neuronal cells of the SCMNs preparation or in primary SCs from sciatic nerve (Fig. 10A, lower panel).

Interestingly, FS3 staining is not uniform, as it appears enriched in discrete domains of the plasma membranes. Likely, this localization may be related to the distribution in patches of neuronal gangliosides, together with sphingolipids and cholesterol (76). These domains are, at least partly, synaptic active zones, as FS3 staining partially co-localizes with the vesicular protein VAMP2 (vesicle associated membrane protein 2) (Fig. 10B).

When combined with NHS (0.5 % v/v), FS3 (0.1 µg/mL) triggers MAC deposition on the surface of SCMNs (Fig. 10C, left panels) and CGNs (Fig. 10C, right panels) as assessed by immune-localization of the C5b-9 epitope on treated neurons.

FS3 and MAC stainings strongly co-localize, particularly in correspondence of varicosities or *bulges* (Fig. 10C, arrowheads, panels at higher magnitude), whose formation occurs rapidly on neurites upon FS3+NHS addition to neurons (see chapter 4.2.2)

No *bulges* nor MAC deposition occur upon FS3+HI-NHS or NHS alone exposure, meaning that the observed effects are anti-GQ1b antibody- and complement- dependent (Fig. 10C).

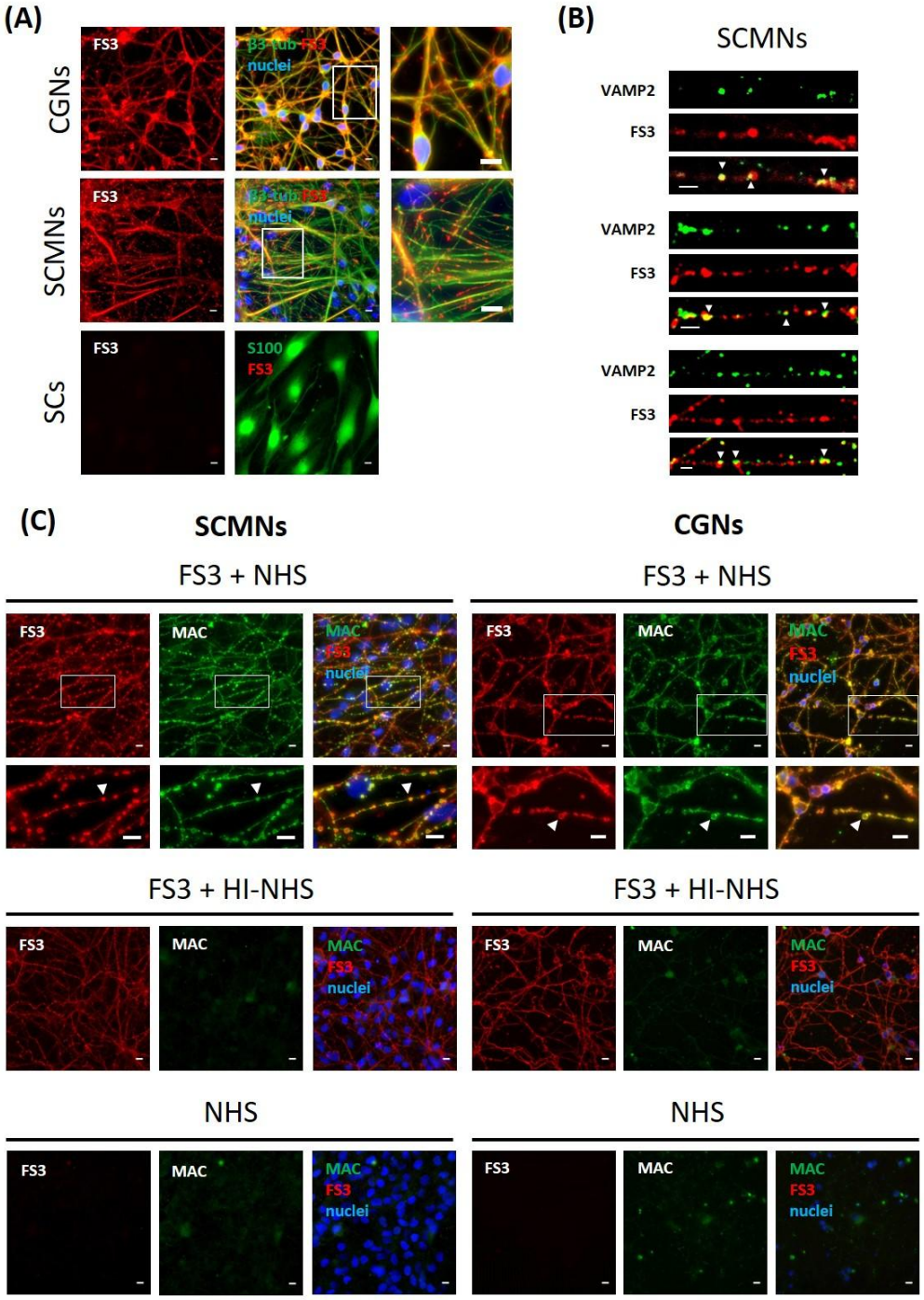

Figure 10: Anti-GQ1b binding and MAC deposition in primary neurons. (A) FS3 (*red*) binding to CGNs or SCMNs (β_3-tubulin positive, *green*) after 20 minutes incubation at 16°C. FS3 punctuated staining is restricted to neuronal cells, as no signal is detectable in SCs (identified by S100 labeling, *green*, lower panels). Nuclei are stained by Hoechst (*blue*). Scale bars: 10 µm. (B) Confocal microscopy shows that FS3 (*red*) partially overlaps at neuronal *bulges* with the presynaptic protein VAMP2 (*green*). Scale bars: 2 µm. (C) FS3+NHS triggers MAC deposition and *bulge* formation in SCMNs (left panels) and CGNs (right panels) upon 20 minutes incubation at 37°C. MAC (*green*) co-localizes with FS3 (*red*) at neuronal *bulges* (*arrowheads*). FS3+HI-NHS or NHS fail to trigger MAC deposition. Nuclei are stained by Hoechst. Scale bars: 10 µm.

4.2.2 MAC assembly mediates Ca^{2+} entry into neurons

As MAC deposition creates pores in neuronal plasma membrane, changes in ions homeostasis are expected to occur. For first we looked at intracellular Ca^{2+} concentration ($[Ca^{2+}]i$): we administered FS3+NHS to neurons loaded with the fluorescent Ca^{2+} indicator Fluo-4-AM, whose fluorescence intensity is directly proportional to Ca^{2+} concentration. In both SCMNs (Fig. 11, left panels) and CGNs (Fig. 11, right panels) the activation of the complement cascade elicited by FS3+NHS leads to a rapid and massive Ca^{2+} influx inside neurons, within 10 minutes in SCMNs and 15 minutes in CGNs from complex addition. No $[Ca^{2+}]i$ changes take place on neurons either upon FS3+HI-NHS exposure, or NHS alone or FS3 alone (Fig. 11A and 11B). $[Ca^{2+}]i$ rise is particularly relevant within *bulges* and neurites (Fig. 11A and 11B). Noteworthy, bulges are sites of maximal MAC deposition, as above reported (Fig.10C).

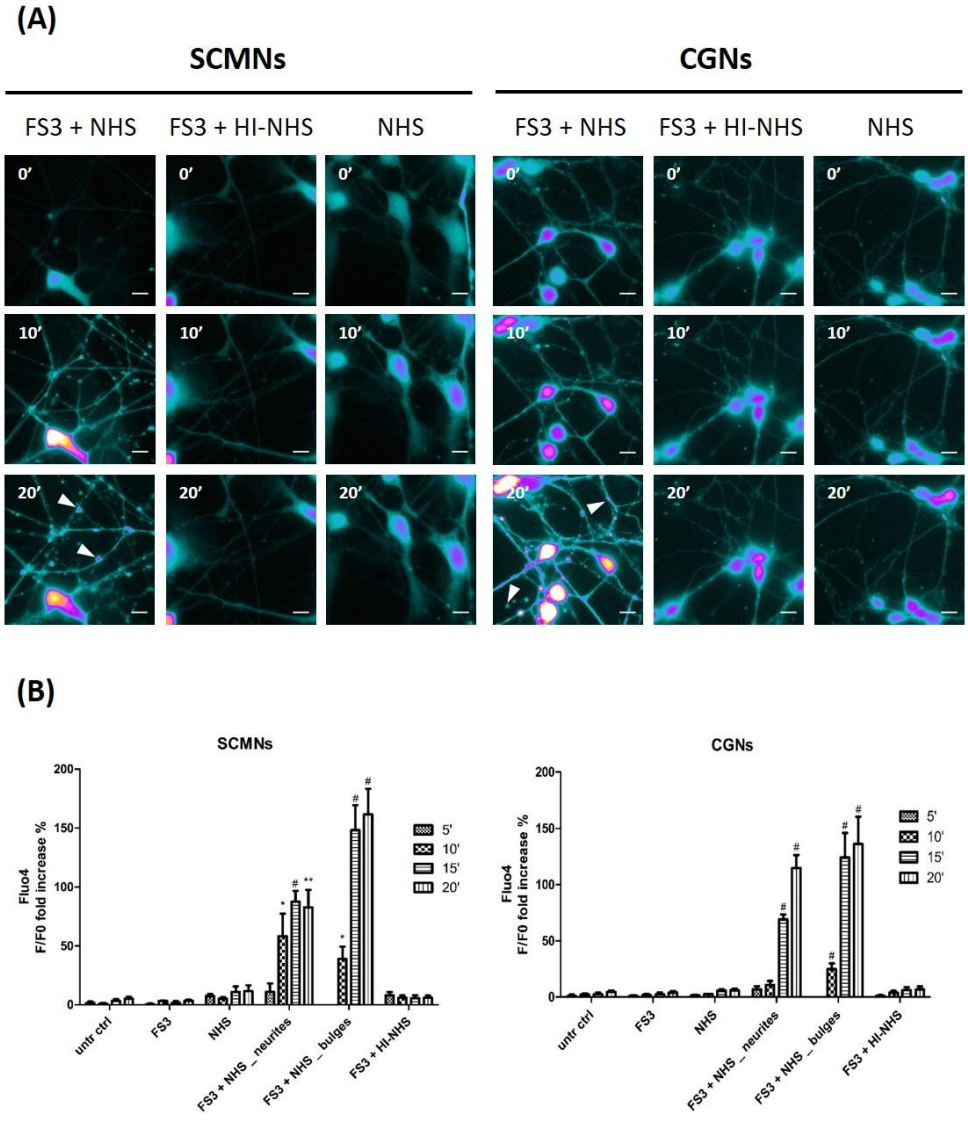

Figure 11: Anti-GQ1b plus complement induces Ca^{2+} influx in cultured neurons. (A) SCMNs (left panels) and CGNs (right panels) loaded with Fluo-4 AM were exposed to FS3+NHS, FS3+HI-NHS, NHS for 20 minutes, and intracellular [Ca^{2+}] calcium changes monitored over time. Images are presented in pseudocolors (*blue*, low calcium; *white*, high calcium). Scale bars: 10 µm. (B) Quantification of selected ROI within neurites. In FS3+NHS samples ROI within *bulges* have been measured. N=3, Student's unpaired *t*-test, two-sides, **p*< 0.05, ***p*<0.01, $^{\#}$*p*<0.001.

4.2.3 Neuronal plasma membrane integrity depends on complement amount

The concentrations of FS3 and NHS employed in this *in vitro* model (0.1 µg/mL and 0.5 % v/v respectively), which are used throughout all the *in vitro* experiments, are the result of a careful analysis on the functional effects of FS3+NHS combination in neurons.

FS3 concentration is sufficient to provide the binding to neuronal surface, as clearly shown by preliminary binding studies of FS3 (Fig. 10A). Concerning NHS, we studied the outcomes of its concentration by Ca^{2+} imaging experiments. Fluo-4 loaded neurons were incubated with a fixed amount of FS3 together with different concentrations of NHS. Representative traces are depicted in Figure 12.

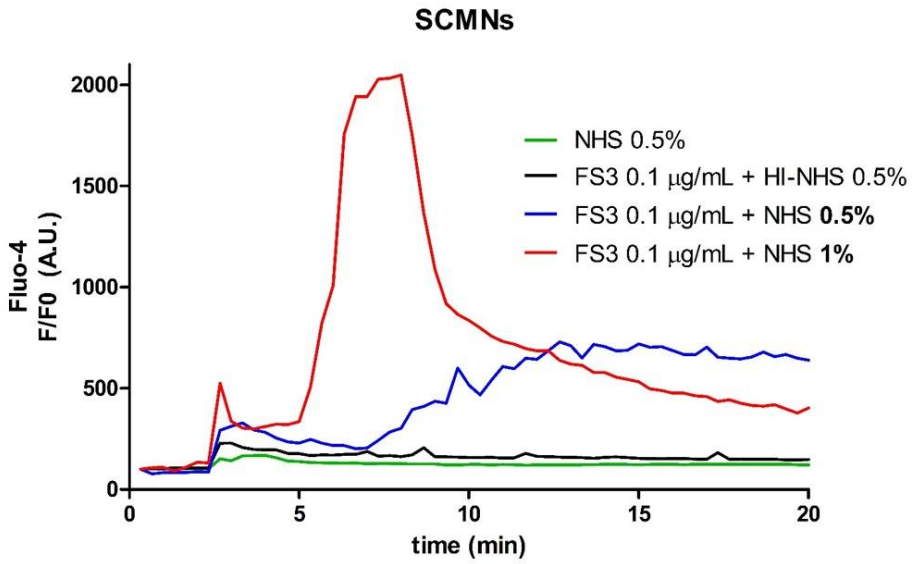

Figure 12: Neuronal plasma membrane integrity depends on NHS concentration. SCMNs loaded with Fluo-4 AM were exposed to FS3 (0.1 µg/mL) *plus* different NHS percentages for 20 minutes (complex added at t=2 minutes). Intracellular calcium levels were measured on selected regions of interest in neurites. Upon FS3+NHS 1% v/v addition (*red trace*), a massive calcium entry takes place in neurons, followed by a rapid decrease in Fluo-4 fluorescence: likely, this is due to the loss of the calcium indicator through a permeabilized plasma membrane. FS3+NHS 0.5 % v/v (*blue trace*) triggers a progressive calcium increase that reaches a *plateu* in around 15 minutes. No calcium changes take place upon incubation with NHS alone (*green trace*) or FS3+HI-NHS (*black trace*). One representative experiment out of 3 experiments is shown.

Upon FS3 *plus* NHS 0.5% v/v incubation (*blue trace*), a progressive rise in $[Ca^{2+}]i$ in SCMNs begins at about 7-8 minutes after addition, reaching in few minutes a *plateau* which is maintained throughout the experiment (20 minutes). NHS concentration reduction (FS3 *plus* NHS 0.2% v/v) has no effects on $[Ca^{2+}]i$ (not shown), meaning that the amount of complement proteins are not sufficient to induce a significant amount of MAC deposition on neuronal surface. Upon doubling of NHS concentration (FS3 *plus* NHS 1% v/v, *red trace*), the rise in $[Ca^{2+}]i$ is definitely much stronger and quicker. However, as soon as $[Ca^{2+}]i$ rapidly reached a peak, it rapidly falls, most likely due to the loss of the Fluo-4 due to plasma membrane permeabilization.

FS3 *plus* NHS 1% v/v can be therefore considered a lytic dose for primary neurons: plasma membrane integrity is not maintained and intracellular content indistinctly flows into the extracellular medium. On the other hand, FS3 *plus* NHS 0.5% v/v still represents a toxic stimulus, but at a sublytic dose: plasma membrane integrity is preserved, neurons are still alive and a series of intracellular responses to the insult are triggered, which are the object of the present study.

In other words, there is an *in vitro* 'effective window' for FS3+NHS treatment: the concentration range of NHS sufficient to elicit a significant, but not lytic, MAC-dependent damage, is very tight.

Taking in account these considerations, FS3 0.1 µg/mL and NHS 0.5% v/v have been adopted in all *in vitro* studies.

Summarizing, NHS concentration (i.e. the quantity of complement proteins), rather than FS3 concentration, is the crucial factor which determines the ultimate fate of FS3+NHS attacked neurons. These findings are in line to those observed in the *in vivo* model.

4.2.4 Anti-GQ1b antibody *plus* complement alters mitochondrial morphology and functionality

Mitochondria are intracellular organelles playing a crucial role in Ca^{2+} handling and buffering. Indeed, mitochondria have been reported to migrate toward cellular sites where Ca^{2+} levels are increased, and the rise in mitochondrial Ca^{2+} concentration closely follows the increase of cytoplasmic $[Ca^{2+}]i$ (77,78). Moreover, mitochondrial dysfunctions have been previously observed in MATs exposed to anti-GQ1b antibodies *plus* complement (36).

As FS3+NHS addition to primary neurons results in a dramatic and rapid $[Ca^{2+}]i$ increase, we speculated that mitochondrial functionality could be affected. To address this hypothesis, we exposed FS3+NHS to neurons loaded with the fluorescent dyes MitotrackerRED or to tetramethylrhodamine methyl ester (TMRM) in order to analyse, respectively, mitochondrial morphology and mitochondrial functionality.

Upon FS3+NHS addition, mitochondria of SCMNs rapidly (within 10 minutes) lose their elongated shape, become rounded and accumulate within *bulges* (Fig. 13A, arrowheads, panels at higher magnitude), which are sites of Ca^{2+} overload (Fig. 11).

Mitochondria within *bulges* are dysfunctional, as they lose rapidly (within 10 minutes) the ability to retain TMRM, indicating loss the mitochondrial membrane potential (Fig. 13B,C). Indeed, under physiological conditions, TMRM is retained within the mitochondrial matrix due to the negative membrane potential across the inner membrane of these organelles, but is lost as soon as the membrane potential collapses due to calcium overload elicited by FS3+NHS or to the uncoupling agent carbonyl cyanide-p-trifluoromethoxyphenylhydrazone (FCCP), employed as a positive control. No morphological nor functional changes took place upon treatment with FS3+HI-NHS or NHS alone (Fig. 13A,B,C). Similar results were obtained also in CGNs (Fig. 13B, lower panel).

Overall, these experiments indicate that the anti-GQ1b antibody *plus* complement represents a defined pathological effector for cultured neurons, where it causes toxicity similar to that occurring *in vivo*, namely deposition of MAC at active zones, followed by Ca^{2+} and mitochondrial homeostasis alterations.

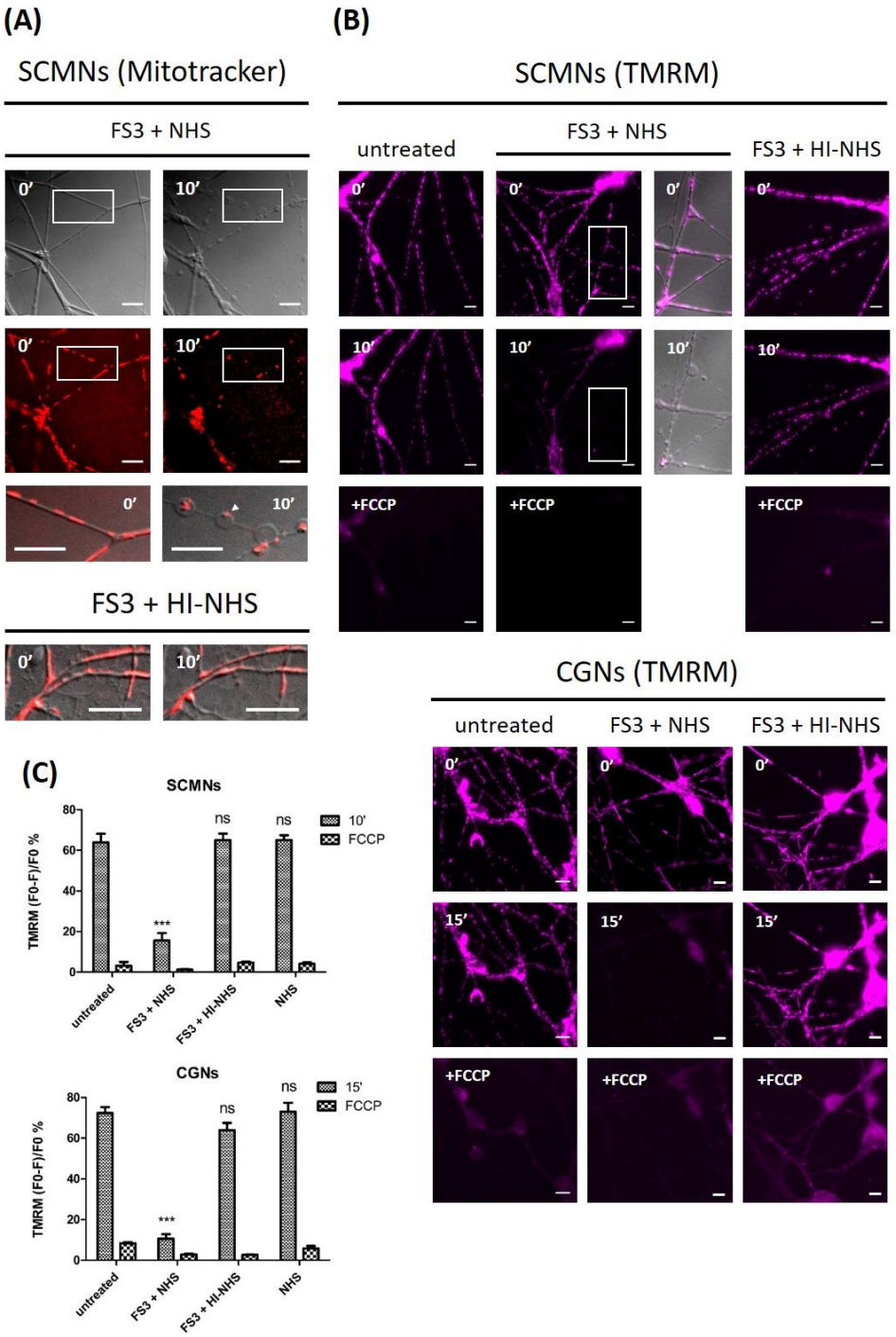

Figure 13: Anti-GQ1b plus complement alters mitochondrial morphology and functionality in cultured neurons. (A) SCMNs were loaded with MitotrackerRed and exposed to FS3+NHS for 10 minutes. Over time mitochondria become rounded and accumulate within *bulges* (arrowheads, lower panels at higher magnification). No changes are detectable when NHS is heat-inactivated. Scale bars: 10 µm. (B) SCMNs (upper panels) and CGNs (lower panels) loaded with TMRM were exposed for 10 (SCMNs) or 15 minutes (CGNs) to saline, FS3+NHS, FS3+HI-NHS or NHS. Mitochondria of FS3+NHS treated neurons progressively lose the dye, indicating an impairment of functionality. No TMRM loss is observed with FS3+HI-NHS or NHS. The complete loss of TMRM is achieved upon FCCP addition (positive control). Scale bars: 10 µm. Quantification performed in regions of interest containing mitochondria is shown in (C). N=3, Student's unpaired *t*-test, two-sides, ***p<0.001.

4.3 Identification of hydrogen peroxide and ATP as *alarmins* driving SCs activation in MFS

4.3.1 Neurons injured by anti-GQ1b antibody *plus* complement produce mitochondrial hydrogen peroxide

High calcium uptake in mitochondria causes the opening of the permeability transition pore and impairs the functionality of the respiratory chain, with production of reactive oxygen species (79,80). Superoxide anion is short lived, as it is rapidly reduced by the mitochondrial superoxide dismutases to hydrogen peroxide (H_2O_2) and oxygen (81). H_2O_2 is relatively stable and represents an ideal intra- and intercellular signaling molecule, as well as a paracrine mediator on neighboring cells, given its permeation through aquaporin channels (82,83).

Accordingly, primary neurons exposed to the pore forming toxin α-LTX produce mitochondrial H_2O_2, with consequent activation of ERK1/2 pathway in SCs, acting therefore as an *alarmin* involved in SCs activation induced by neurodegeneration (18).

To test whether H_2O_2 is produced inside neurons also upon FS3+NHS exposure, we took advantage of two specific H_2O_2 specific probes with different cellular localization, PF6-AM (cytoplasmic) and MitoPY1 (mitochondrial), kindly given by Prof. Chang (University of California) (29,62). PF6-AM takes advantage of multiple masked carboxylates to increase cellular retention, and hence sensitivity to low levels of peroxide. In its ester-protected form, PF6-AM can readily enter cells: once in the cytosol, the protecting group are rapidly cleaved by intracellular esterases to produce their anionic carboxylate forms, which are effectively trapped within cells. MitoPY1, on the other hand, is a bi-functional molecule that combines a chemoselective boronate-based switch and a mitochondrial-targeting phopshonium moiety for the detection of H_2O_2 in mitochondria.

When exposed to FS3+NHS, primary neurons progressively produce H_2O_2, as shown by increase of PF6 fluorescence emission in live imaging experiments (Fig. 14A).

Noticeably, $[Ca^{2+}]i$ increase and H_2O_2 generation spatially and temporally correlate. Indeed H_2O_2 production takes place with a time course superimposable to that of $[Ca^{2+}]i$ increase, particularly in correspondence of neuronal *bulges* (Fig. 14A, arrowheads and 14B), which are sites of Ca^{2+} entry and dysfunctional mitochondria accumulation. Mitochondria are the main source of H_2O_2, as revealed by experiments on MitoPY1 loaded CGNs exposed to FS3+NHS (Fig. 14C).

H_2O_2 production is FS3- and complement- dependent, as it is not detectable upon exposure to FS3+HI-NHS, or NHS alone, or FS3 alone (Fig. 14A,B).

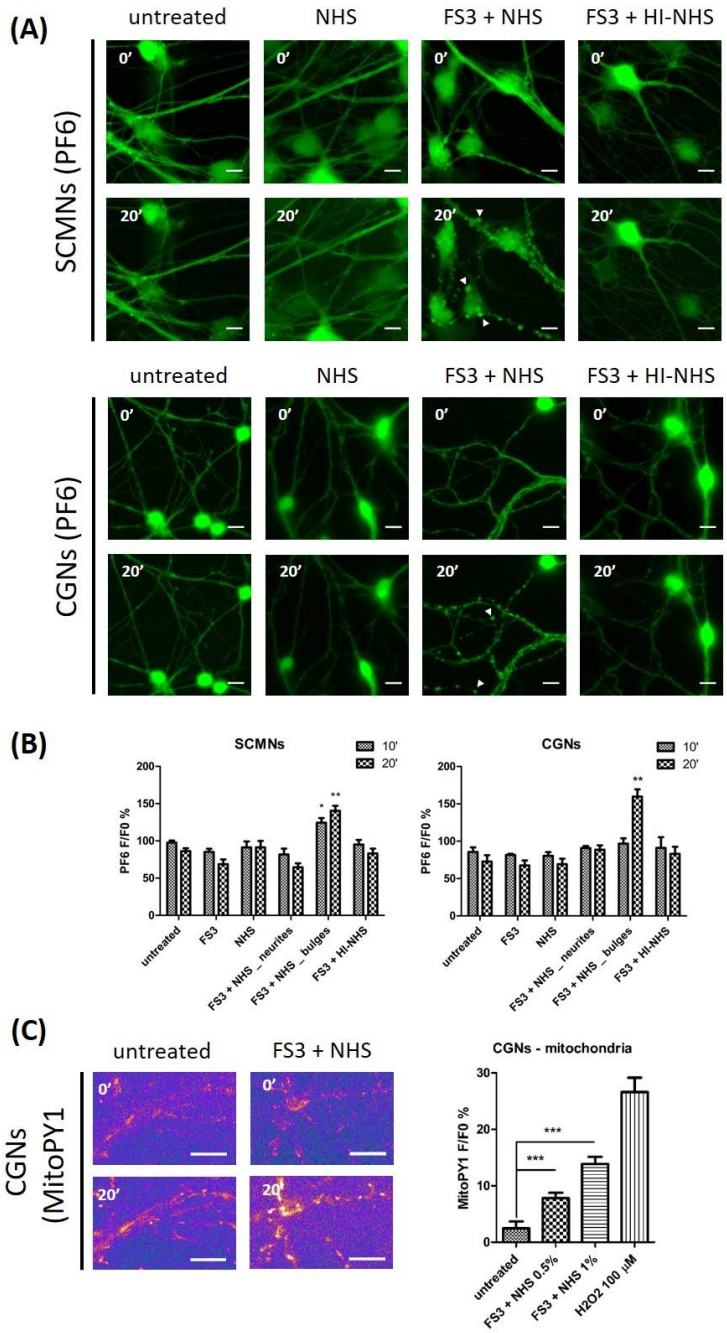

Figure 14: Anti-GQ1b plus complement triggers mitochondrial hydrogen peroxide production in primary neurons. (A) SCMNs (upper panels) and CGNs (lower panels) loaded with the cytosolic H_2O_2 probe PF6-AM were exposed to saline, FS3+NHS, NHS, FS3+HI-NHS, for 20 minutes, and changes in fluorescence were measured over time. Scale bar: 10 µm. Quantification of H_2O_2 production at the level of neurites and *bulges* (*arrowheads*) is shown (B). N≥4 independent experiments for each condition, Student's unpaired *t*-test, two-sides, **p*<0.05, ***p*<0.01. (C) Hydrogen peroxide is produced inside mitochondria of CGNs loaded with the mitochondrial-targeted H_2O_2-sensitive probe MitoPY1. Hydrogen peroxide (100 µM) was used as positive control. N=3, Student's unpaired *t*-test, two-sides, ****p*<0.001.

4.3.2 Anti-GQ1b antibody *plus* complement activates ERK1/2 pathway in Schwann cells co-cultured with neurons

Growing evidence indicate that H_2O_2 is an important intercellular signaling molecule regulating kinase-driven pathways (84,85). It triggers ERK phosphorylation in different cell types with consequent activation of downstream gene transcription. ERK1/2 signaling pathway was recently shown to play a central role in the orchestration of axon repair by SCs (31), and ERK1/2 becomes phosphorylated in PSCs of αLTX- intoxicated mice (18). Activated SCs then actively participate to the process of nerve terminal regeneration after NMJ damage. With these considerations in mind, we wonder whether H_2O_2 could act as a signaling molecule and activate ERK1/2 signaling pathway also in the present model of MFS.

As FS3 binds selectively to neurons and not to SCs (Fig. 10A), MAC is not deposited in SCs. Therefore, FS3+NHS represents a specific tool to deliver MAC exclusively to neurons in co-cultures with SCs. However, NHS is not only a 'donor' of complement proteins at physiological concentrations, but also a source of a huge number of molecules of different types (growth factors, hormones, IgGs …). This implies that one or more of these NHS components could activate by themselves cellular pathways in SCs (as well as in neurons) in a MAC-independent way, therefore biasing the purpose of the experiment. Hence, whatever neuron-SCs signaling is being investigated, the NHS alone condition must be included in each experiment, together with other appropriate negative controls.

We tested ERK phosphorylation in co-cultures of primary neurons and SCs exposed to FS3+NHS for 30 minutes, and detected phospho-ERK (p-ERK) in SCs by western blot (Fig. 15A,B) and immunofluorescence (Fig. 15C). ERK phosphorylation is MAC-dependent, as NHS alone (as well as FS3+HI-NHS) fails to trigger any p-ERK in co-cultured SCs.

The addition of catalase, a H_2O_2-inactivating enzyme, in the extracellular medium significantly reduced ERK phosphorylation in SCs (Fig. 15A,B), indicating that H_2O_2 is an important contributor of ERK1/2 activation.

No p-ERK increase was detected neither in isolated neurons (Fig. 15A,B) nor in neurons in co-cultures (Fig. 15C) upon exposure to FS3+NHS, indicating that SCs are indeed the source of p-ERK.

Altogether, these experiments demonstrate that H_2O_2 is produced by neurons in this model of MFS and represents an *alarmin* which activates SCs.

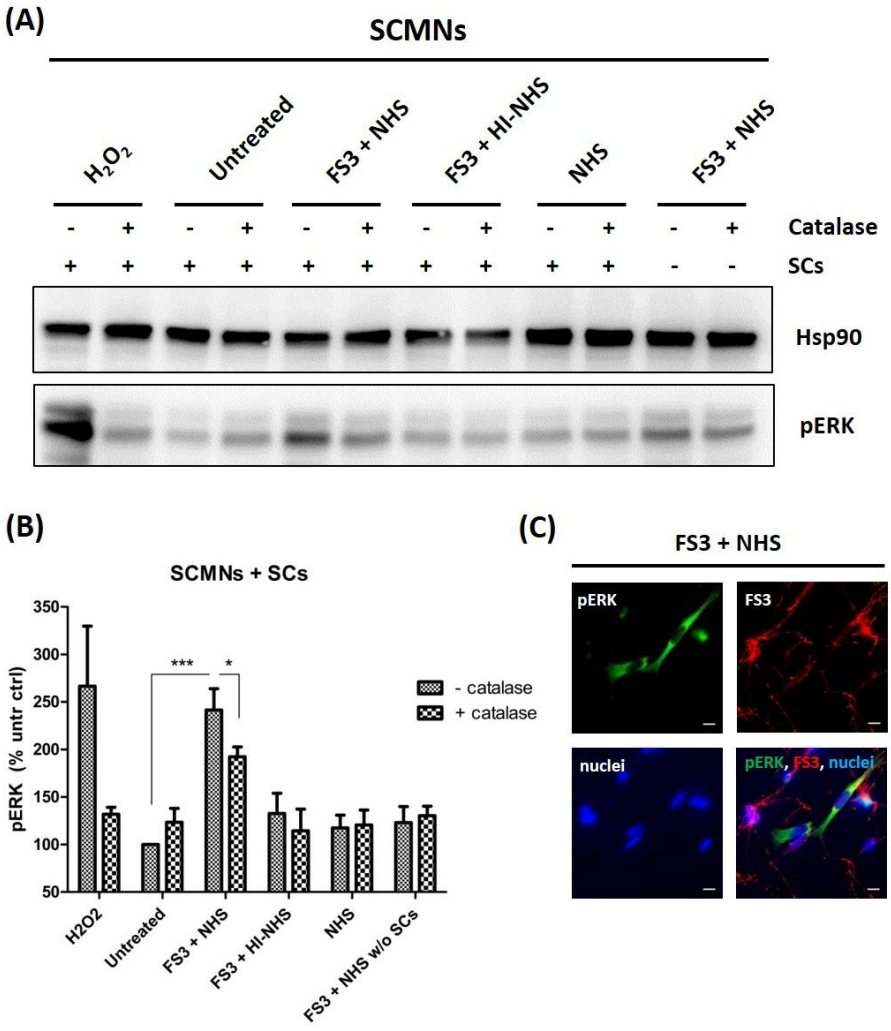

Figure 15: Anti-GQ1b plus complement induces ERK1/2 phosphorylation in SCs co-cultured with neurons. (A) Representative Western blot showing ERK phosphorylation induced by 30 minutes incubation with FS3+NHS in SCs co-cultured with SCMNs. Phospho-ERK levels are reduced upon pre-incubation with catalase. No ERK activation is detected following exposure to NHS or when NHS is heat-inactivated. FS3+NHS fails to increase p-ERK levels in isolated SCMNs. (B) Quantification of p-ERK levels normalized on Hsp90 signal. N=5, Student's unpaired *t*-test, two-sides, **p*<0.05, ****p*<0.001. (C) Phospho-ERK signal (*green*) is restricted to SCs in neurons-SCs co-cultures treated with FS3+NHS for 30 minutes, in line with Western blot results. Neurons are identified by FS3 staining (*red*). Nuclei are stained by Hoechst (*blue*). Scale bars: 10 µm.

4.3.3 ATP is released by neurons after anti-GQ1b antibody *plus* complement attack

Beside its known role as energy source, ATP is also an extracellular messenger acting on different types of purinergic receptors. ATP is an important signalling molecule in the PNS, where it plays important roles in the chemical communication between MAT and PSCs (5,34).

Recent work in our laboratory demonstrated that ATP released by α-LTX injured neurons activates different cellular pathways in SCs (24). We therefore aimed to analyze the role of ATP as potential *alarmin* released by MAC-damaged neurons.

As a first evidence, we found that primary neurons exposed to FS3+NHS rapidly release ATP in the extracellular medium, measured by a luminometric assay, peaking at 10 minutes in SCMNs and at 15 minutes in CGNs (Fig. 16A). This slight temporal difference is likely due to the small (but reproducible) difference in the time needed for MAC deposition by FS3+NHS at SCMNs and CGNs, as shown by Ca^{2+} imaging experiments presented above (Fig. 11B). ATP release is FS3- and complement- dependent, as it is not detectable upon exposure to NHS alone or to FS3+HI-NHS.

Under the same experimental conditions, no lactate dehydrogenase activity (LDH) was measured in the cell supernatant (Fig. 16B), meaning that ATP is not released as a mere consequence of cell lysis, as membrane integrity is preserved upon FS3+NHS treatment. An active mechanism of ATP release is therefore triggered in neurons after FS3+NHS injury.

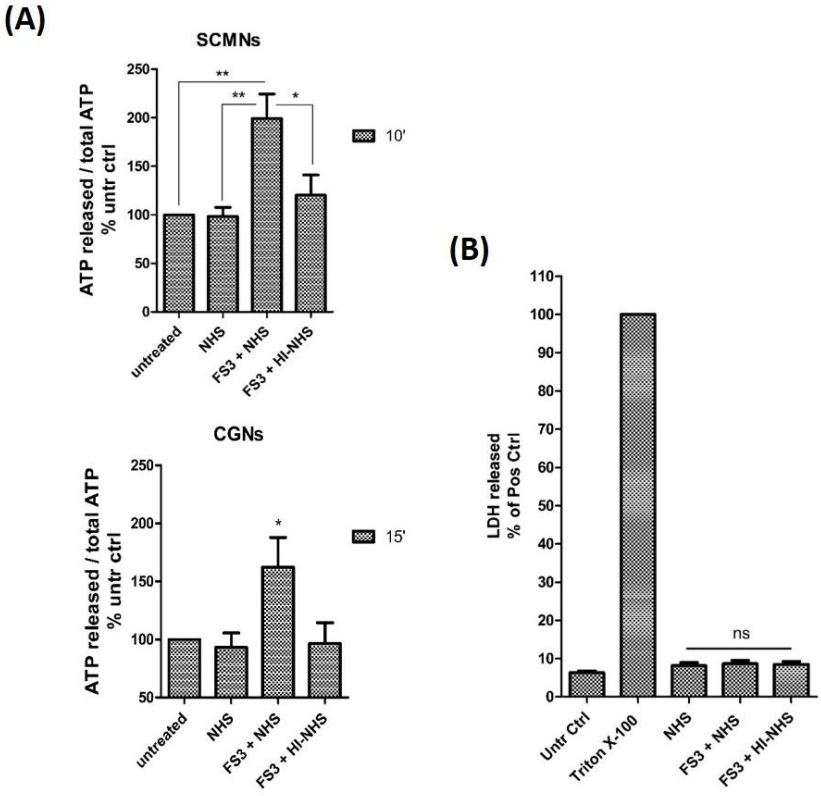

Figure 16: ATP is released by neurons treated with anti-GQ1b antibody plus complement. (A) Time-course of ATP release by SCMNs and CGNs exposed to NHS, FS3+NHS, or to FS3+HI-NHS for 10 (SCMNs) or 15 minutes (CGNs). The amount of the release is expressed as percentage of total ATP relative to untreated samples. *P < 0.05; **P < 0.01. N=7 (Student's t test, unpaired, two-side). (B) Lactate dehydrogenase (LDH) activity measured in the supernatant of CGNs treated as in (A), and expressed as percentage of TRITON X-100 (0.5% v/v) treated samples. ns= not significant.

4.3.4 Neuronal ATP triggers calcium spikes in Schwann cells

As mentioned before, ATP can activate different types of purinergic receptors at PSCs surface, and one possible consequence is the elevation of $[Ca^{2+}]i$ in PSCs (5).

We thus wondered whether SCs might sense and respond to ATP derived from MAC-injured neurons, and investigated the intracellular pathways thereby activated. We previously observed that primary SCs respond to exogenous ATP with cytosolic Ca^{2+} spikes (24).

When SCMNs-SCs or CGNs-SCs co-cultures, loaded with the Ca^{2+} indicator Fluo-4-AM, are exposed to FS3+NHS, Ca^{2+} spikes are observed in SCs immediately after the formation of bulges in neuritis and elevation of $[Ca^{2+}]i$ in neurons (Fig. 17A). No Ca^{2+} changes occur under control conditions and upon exposure to NHS alone or to FS3+HI-NHS (Fig. 17B). Noteworthy, a Ca^{2+} spike in SCs is observed in all samples upon NHS addition (independently on heat inactivation), which is likely to be due to the quick and transient action of unknown component(s) of human serum. Preincubation of co-cultures with apyrase, an enzyme which hydrolyses ATP to AMP and inorganic phosphate, strongly reduces FS3+NHS induced Ca^{2+} spikes in SCs in co-cultures (Fig. 17C), providing evidence that ATP is indeed an *alarmin* which engages Ca^{2+} signaling in SCs also in this model of MFS.

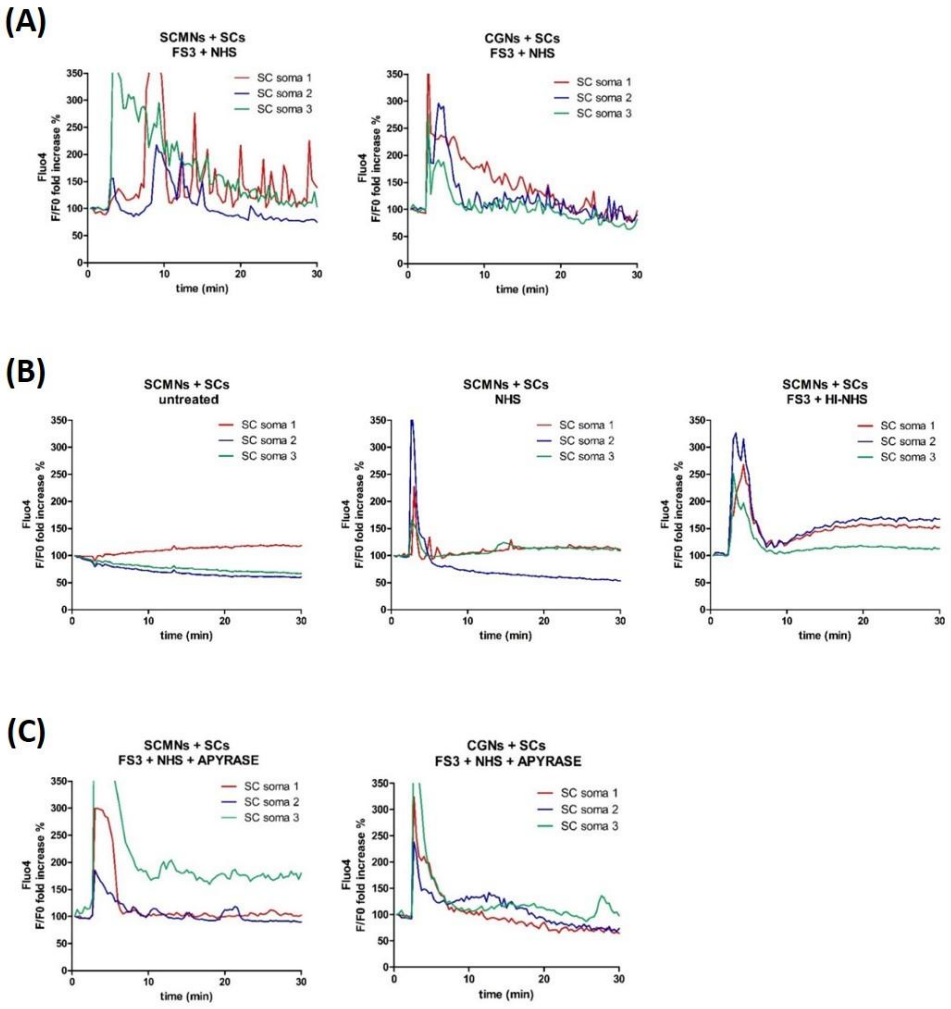

Figure 17: Neuronal ATP triggers calcium spikes in Schwann cells in co-cultures treated with anti-GQ1b antibody plus complement. Co-cultures of primary SCs and SCMNs or CGNs were loaded with Fluo-4 AM and exposed to FS3+NHS, NHS, FS3+HI-NHS, or saline for 30 minutes. Intracellular calcium changes are represented in a pseudocolor scale (*blue*: low concentration; *white*: high concentration), and quantified. (A) In co-cultures exposed to FS3+NHS calcium spikes are observed in SCs. (B) No calcium increase is detectable in SCs upon incubation with saline, NHS, or FS3+HI-NHS. (C) Apyrase preincubation nearly abolishes calcium spikes in SCs. Representative traces are reported. N=3.

4.3.5 Cyclic AMP is produced by Schwann cells in response to anti-GQ1b plus complement neuronal injury

Among the intracellular pathways through which purinergic receptors can transduce the extracellular ATP input (33), we investigated the possible involvement of the second messenger cyclic AMP (cAMP), whose production is elicited by type P2Y purinergic receptors activation. Primary SCs respond to exogenous ATP by raising their cAMP content (24). Accordingly, cAMP levels were imaged in SCs in neurons-SCs co-cultures transfected with a new generation *Epac* probe (63) before and after exposure to FS3+NHS (Fig. 18). Within few minutes from FS3+NHS addition a cAMP rise in SCs is evoked, with a peak at about 8-10 minutes in SCMNs-SCs co-cultures and 12-15 minutes in CGNs-SCs co-cultures, then returning to basal levels.

The positive control forskolin was added at the end of the experiment to reach maximum signal. No changes in cAMP levels were detected with saline alone, NHS or FS3+HI-NHS.

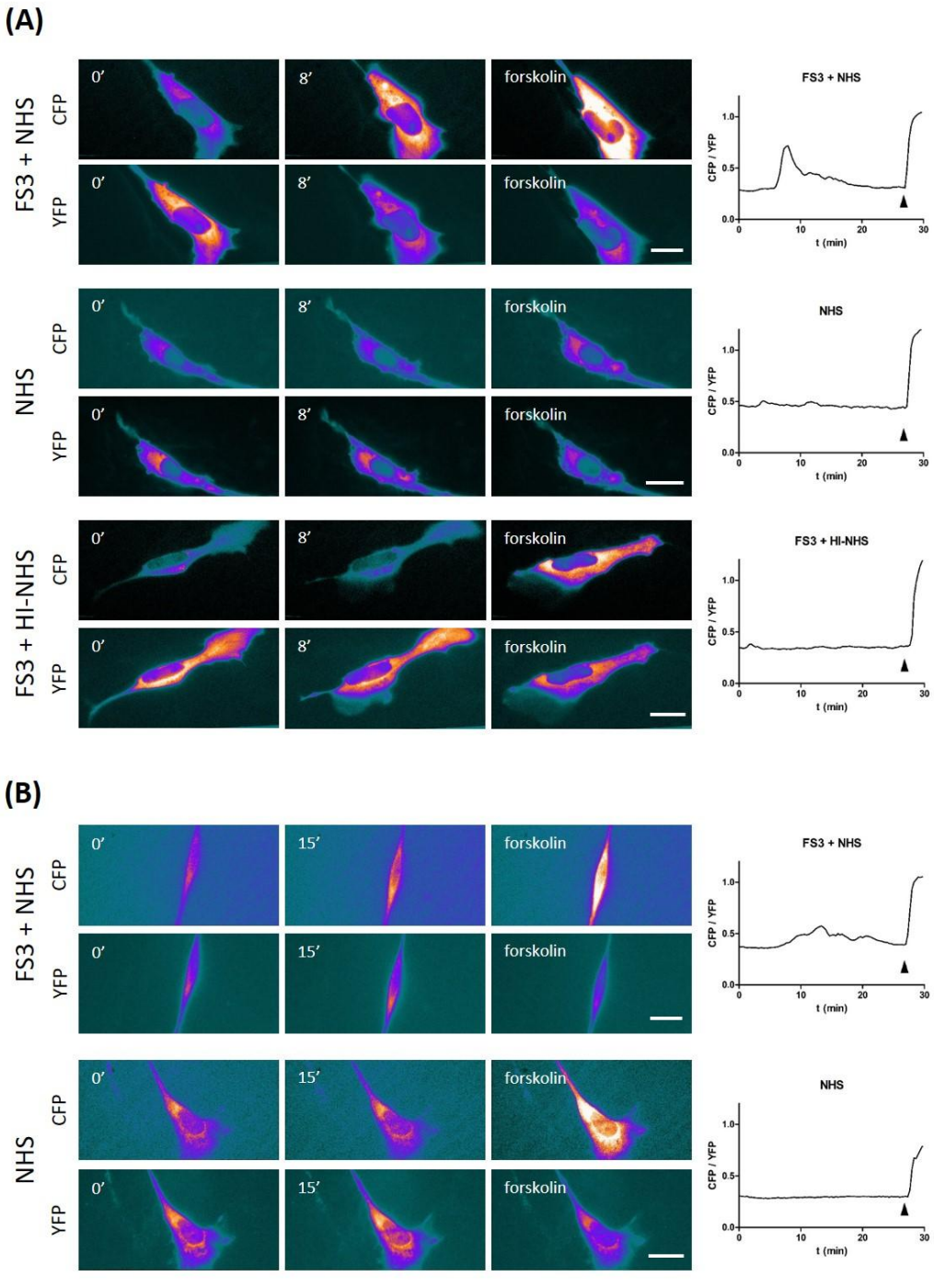

Figure 18: Cyclic AMP is produced in Schwann cells in co-cultures upon FS3+NHS treatment. SCs in co-cultures with SCMNs (A) or CGNs (B) were transfected with the EPAC H187 sensor and FRET measured during exposure to FS3+NHS (complex added at t=1 minute), NHS or FS3+HI-NHS. Forskolin was added at the end of the experiment (t=28 minutes, arrowhead) as positive control. FRET causes a decrease in YFP fluorescence and a parallel increase in CFP intensity, as indicated by the pseudocolor images (*blue*: low fluorescence; *white*: high fluorescence). Quantification is shown in the right panels, where FRET (CFP/YFP) is expressed as the ratio between the background-corrected donor (CFP) and acceptor (YFP) signals.

4.3.6 Neuronal ATP induces CREB phosphorylation in Schwann cells

Activation of both ERK 1/2 and cAMP pathways promote the transcriptional activity of CREB, one of the best understood phosphorylation-dependent transcription factors, involved in a variety of cellular processes and in neuron-glia communication (86). As both pathways are engaged in SCs co-cultured with MAC injured neurons (Fig. 15,18) and CREB becomes phosphorylated in isolated SCs exposed to ATP (24), it is well conceivable that CREB might be activated also in this MFS model. This is the case, as showed by immunofluorescence experiments on SCMNs-SCs co-cultures, which reveal an increase in phospho-CREB (Ser133) (pCREB) signal in SCs (S100-positive cells) nuclei after 10 minutes of FS3+NHS incubation (Fig. 19A,B). CREB activation is anti-GQ1b antibody and complement dependent, as it is not detectable if co-cultures are exposed to NHS alone or FS3+HI-NHS. Furthermore, it is extracellular ATP dependent, as preincubation with apyrase abolishes CREB phosphorylation. These results were further validated by western blot (Fig. 19C,D). Interestingly, FS3+NHS incubation of co-cultures for longer times (15 and 30 minutes) failed to produce any detectable pCREB signal. This can be due to the presence of a negative feedback system in SCs that assure the return to basal CREB activity once engaged, and that is probably involved also in the reversibility of FS3+NHS dependent cAMP elevation observed in FRET experiments (Fig. 18).

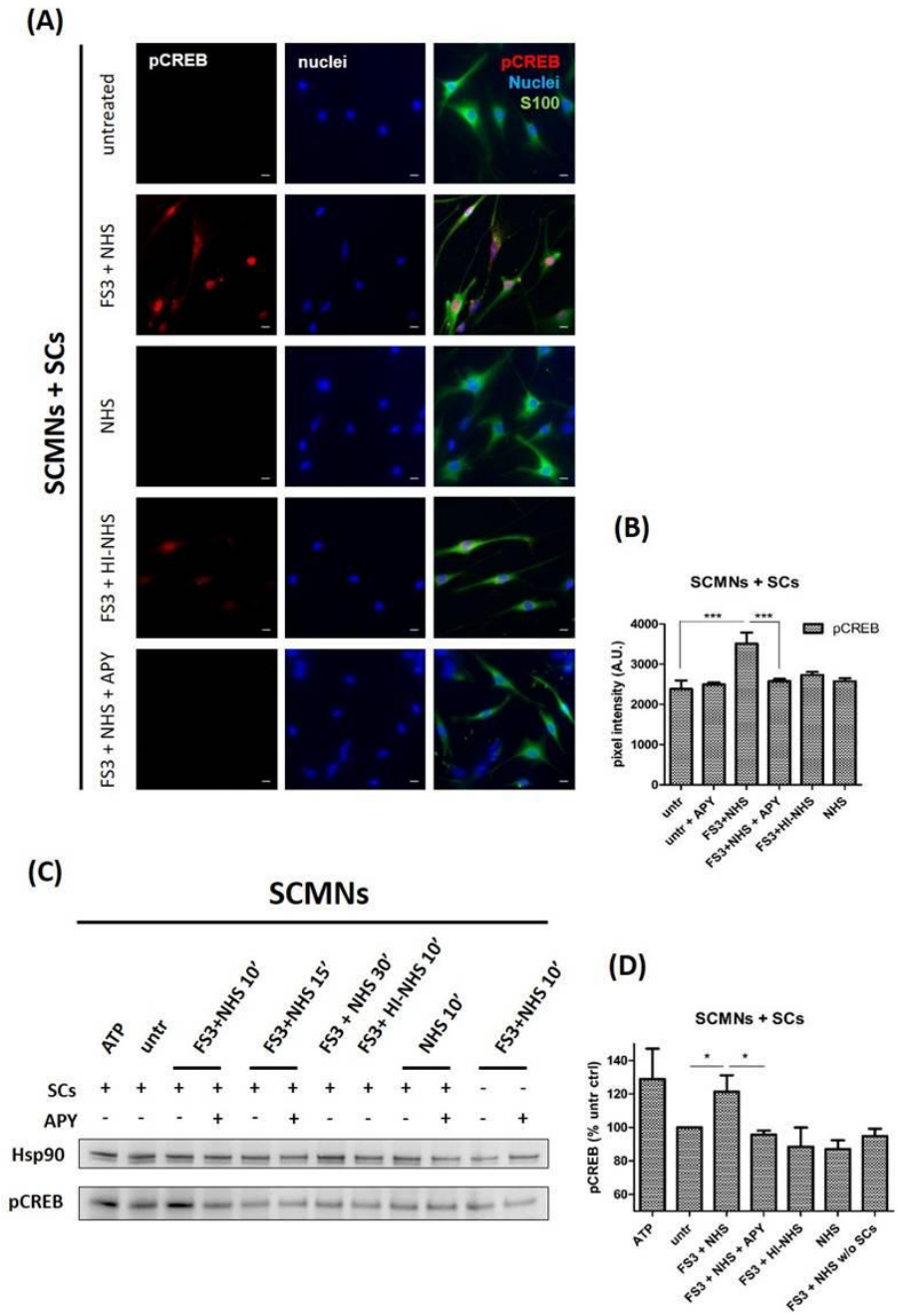

Figure 19: Neuronal ATP induces CREB phosphorylation in Schwann cells co-cultured with neurons treated with anti-GQ1b antibody plus complement. (A) Immunofluorescence of SCMNs-SCs co-cultures exposed for 10 minutes to saline, FS3+NHS, NHS, FS3+HI-NHS, or FS3+NHS *plus* apyrase. SCs are S100-positive (*green*), phospho-CREB is detected by a specific antibody (*red*), nuclei are stained by Hoechst (*blue*). Scale bars: 10 µm. (B) Quantification of phospho-CREB and S100 -positive cells. ***P<0.001. N=3. (C) Representative Western blot showing phospho-CREB levels in SCMNs-SCs co-cultures exposed to FS3+NHS for 10, 15 and 30 minutes, and its reduction by apyrase. After 10 minutes incubation, phospho-CREB signal is significantly higher in FS3+NHS samples with respect to untreated co-cultures, and this increase is inhibited by apyrase. ATP 100 µM is used here as positive control. No phospho-CREB is detectable in neurons exposed to FS3+NHS, demonstrating that phospho-CREB signal in co-culture lysates derives from SCs. Quantification is shown in (D). Band intensities of samples treated for 10 minutes are normalized to the housekeeping Hsp90 and expressed as percentage of the untreated control. *P<0.05. N=4 (Student's t test, unpaired, two-side).

5. DISCUSSION

Many efforts were made by the scientific community in the last 100 years following the first observations by Guillain and Barré in 1916, in order to shed light on the biological processes that underline GBS variants, including MFS. To date, many question marks are still unsolved. Much of the present research aims at unraveling the pathogenic mechanisms leading to neurodegeneration, but the molecular players that participate in neuroregeneration and neurotransmission recovery are ill-known. We opted to study MFS, which is the GBS variant with the higher percentage of complete recovery, in order to dissect the molecular signaling taking place between MAT and PSCs driving nerve terminal regeneration.
In particular, I wondered which are the alarm signals (*alarmins*) produced by the degenerating MAT.

To achieve this goal, I set-up an *in vivo* model of MFS, characterized by minimal invasiveness. The injection of an anti-GQ1b/GT1a monoclonal antibody FS3 *plus* NHS as a source of complement in living mice induces an acute and highly reproducible MAT degeneration, whose complete regeneration takes few days. This model represents an appropriate and controlled system to dissect the molecular mechanisms underlying degeneration and regeneration of peripheral nerve terminals, and to define the PSCs contribution to these processes.

FS3 displays the same affinity to GQ1b and GT1a gangliosides (46), so it cannot be distinguished whether its effects at the NMJ (and in primary neurons) are mediated by its binding to GQ1b, or GT1a, or both. Notably, the binding of autoantibodies to both gangliosides is implicated in MFS pathogenesis, although anti-GQ1b reactivity is the most frequent serological hallmark of the disease (49,50).

Noteworthy, FS3+NHS effects vary markedly, depending on the muscles employed (LAL or soleus muscles). On one hand, MAT degeneration in LAL muscles occurs rapidly (within 3-4 hours), with neuroregeneration accomplished within 3 days, but only a fraction (about 60%) of total NMJs are affected. On the other hand, in soleus muscles FS3+NHS induced MAT degeneration is nearly total (more than 90% NMJs degenerated), but takes longer to occur (NMJ neurodegeneration peaks at 2 days after injection). Such discrepancies may rely on differences in muscle fibres composition

between soleus muscle (nearly all slow fibres) and LAL muscle (compresence of slow and fast fibres). Previous works reported a remarkable resistance of LAL NMJs, in comparison to soleus muscle, to neurodegeneration induced by G93A mutation in the SOD1 protein (linked to amyotrophic lateral sclerosis), and to age-related alterations of endplate morphology (87).

The fate of the endplate upon MAC deposition depends on complement resistance mechanisms of the MAT. It is well known that susceptibility to complement attack can vary in different kind of cells. One single MAC channel is sufficient to induce the lysis of one single erythrocyte (88). On the other hand, other cell types display an array of plasma membrane and cytoplasmic proteins which protect the cells from MAC damage.

The first line of defense is represented by plasma membrane bound proteins, such as CD46, CD55 and CD59, which are complement proteins receptors present in nearly all tissues, which interfere with the activation of the complement cascade, therefore blocking MAC deposition at self-tissues (52).

A second line of defence is activated once MAC is deposited at plasma membrane, and consists of the activation of intracellular processes to limit cellular damage. A consistent line of research is actively studying the processes of membrane repair following different types of wounding: however the different cell types employed (skeletal muscle cells are the most studied because the most subjected to plasma membrane damage), the types of insults employed (scratch, compression, laser beam wounding, pore forming toxins, MAC), and the proteins/pathways involved (dysferlin, SNARE proteins, calpains, annexins, ESCRT proteins; exocytosis, endocytosis, blebbing, …) make the understanding of the cellular events that protect the MAT from sublytic MAC very challenging (89).

Despite these difficulties, it is widely accepted that resistance to complement lysis is achieved by the physical removal of MAC by both endocytic and exocytic process. Pioneer studies by Morgan and collegues demonstrated that polymorphonucleated leukocytes are able to get rid of MAC by emission of MAC-loaded vesicles, and at the same time, by endocytosis of MAC and subsequent degradation of its components inside the cell (90,91).

Whether one of more of the abovementioned protective mechanisms are engaged at MAT upon MAC deposition in the present MFS model is an open question. As MAC is deposited at MAT *in vivo* also at 'sublytic' doses (FS3 10 µg + NHS 50 % v/v in 15 µL of injection volume), it is likely that the first line of defence, represented by complement regulatory proteins on the plasma membrane, if present, is overwhelmed. It is reasonable that MAT is able to engage one or more

cellular mechanisms in order to physically remove the deposited MAC. In the presence of a higher quantity of complement proteins recruited to the presynaptic membrane (i.e FS3 10 µg + NHS 50 % v/v in 100 µL of injection volume), also these mechanisms are overwhelmed and neurodegeneration takes place.

In parallel to the *in vivo* MFS model, I set-up an *in vitro* MFS model, consisting of primary neurons exposed to FS3 *plus* NHS, which well replicates the pathogenic effects of anti-GQ1b antibodies *plus* complement at the NMJ, i.e. deposition of MAC, massive Ca^{2+} overload inside neuronal cytoplasm and impairment of mitochondrial functionality.
I observed the appearance of plasma membrane swelling (*bulges*) in neurites. Neuronal *bulging* is likely to be driven by the following mechanisms: i) massive and uncontrolled Ca^{2+}-induced release of synaptic vesicles, not counterbalanced by synaptic vesicle recycling, resulting in membranes surplus at the neurites surface. Indeed, bulges are sites of vesicular marker VAMP2 accumulation (Fig. 10B); ii) cytoskeletal and actin degradation caused by Ca^{2+}-activated proteases, which renders the overlying plasma membrane devoid of structural support; iii) an osmotic imbalance derived from large proteins and other osmotically active intracellular components, that cannot permeate through the complement pores.

By this simplified (but relevant) *in vitro* approach we identified two *alarmins*, H_2O_2 and ATP, which are released by neurons upon FS3+NHS attack.
Mitochondrial ROS production increases under many stress conditions. Hydrogen peroxide is one of the most stable ROS species, and can permeate across cellular membranes through aquaporins-mediated extracellular transport (82), therefore acting as a paracrine signal. Once inside the target cell, H_2O_2 can act as second messenger via chemo-selective oxidation of cysteine residues in signalling proteins (93,94).

ATP is long-known as an important alarm molecule. It signals through purinergic receptors, whose activation elicits different signalling pathways in target cells including Ca^{2+}, cAMP, inositol-1,4,5-triphosphate, phospholipase C and others (32,33). PSCs express purinergic receptors and respond with Ca^{2+} elevations to ATP released by MAT during high frequency stimulation (5).
We reported that ATP release from neurons in the present model of MFS is not mediated by alterations of plasma membrane integrity, as the FS3+NHS concentrations adopted *in vitro* were

non-lytic (see chapter 4.2.3)**,** as confirmed by LDH assay (Fig. 16B). The exact mechanism of ATP release has not been examined. It is likely that one or more of the following mechanism are implicated: i) exit from MAC pores, given that ATP has a small radius (6 Å) (92), and it may pass through the large MAC pore (110 Å); ii) exit through the massive synaptic vesicles release induced by Ca^{2+} influx; iii) non-synaptic, non-vesicular ATP exit through volume-activated anion channels (VAACs) activated by microscopic axon swelling during action potential firing induced Ca^{2+} entry (92); iv) transient lipidic pores generated by the activation of phospholipases A2 and formation of lysophospholipids and fatty acids.

In neurons-SCs co-cultures MAC deposit is restricted to neuronal membranes, thanks to FS3 specificity, and this event is followed by the activation of ERK1/2 and CREB pathways, Ca^{2+} spikes and cAMP synthesis in SCs. We demonstrated that these effects depend on H_2O_2 and ATP released by neurons. Indeed, preincubation of co-cultures with catalase, a H_2O_2-inactivating enzyme, prevented the activation of ERK1/2 pathway in SCs. Noteworthy, ERK1/2 activation was not completely abolished by catalase, indicating that other mediators are involved.

Preincubation of co-cultures with apyrase, an enzyme which cleaves ATP to adenosine and inorganic phosphates, prevented Ca^{2+} spikes and CREB phosphorylation. Both catalase and apyrase are tetramers of high molecular weight, respectively 250 kDa and 200 kDa, and are not internalized inside cells. Therefore, they exert their catalytic activity only in the extracellular medium, further supporting that the H_2O_2 and ATP are released by the MAC-attacked neurons in the extracellular medium in neurons-SCs co-cultures, where they are sensed by SCs, thus engaging molecular pathways important for nerve regeneration (Fig. 20).

Indeed, following *cut and crush* nerve injury, myelinating SCs respond to axonal damage with a strong, sustained activation of the Raf/MEK/ERK signalling pathway, and this response was found to play a central role for the orchestration of the repair response (31,95). Furthermore, given the involvement of cAMP as an important second messenger regulating phagocytosis (96), this signalling cascade may be important for PSCs as well, as these cells display macrophagic-like properties after MAT degeneration (18,36). Synthesis of cAMP can lead to activation of CREB, a master transcription factor regulator of cell responses to a vast array of extracellular stimuli, including neurotransmitters, hormones, growth factors, synaptic activity, stressors, and inflammatory cytokines (97).

To conclude, the MFS model presented here has allowed to better elucidate the cross-talk between neurons and SCs, and to identify alarm signals driving nerve regeneration. This and future studies might provide a deeper understanding of the molecular mechanisms underlying neuroregeneration in MFS and, likely, of other MAT-affecting neurodegenerative pathologies.

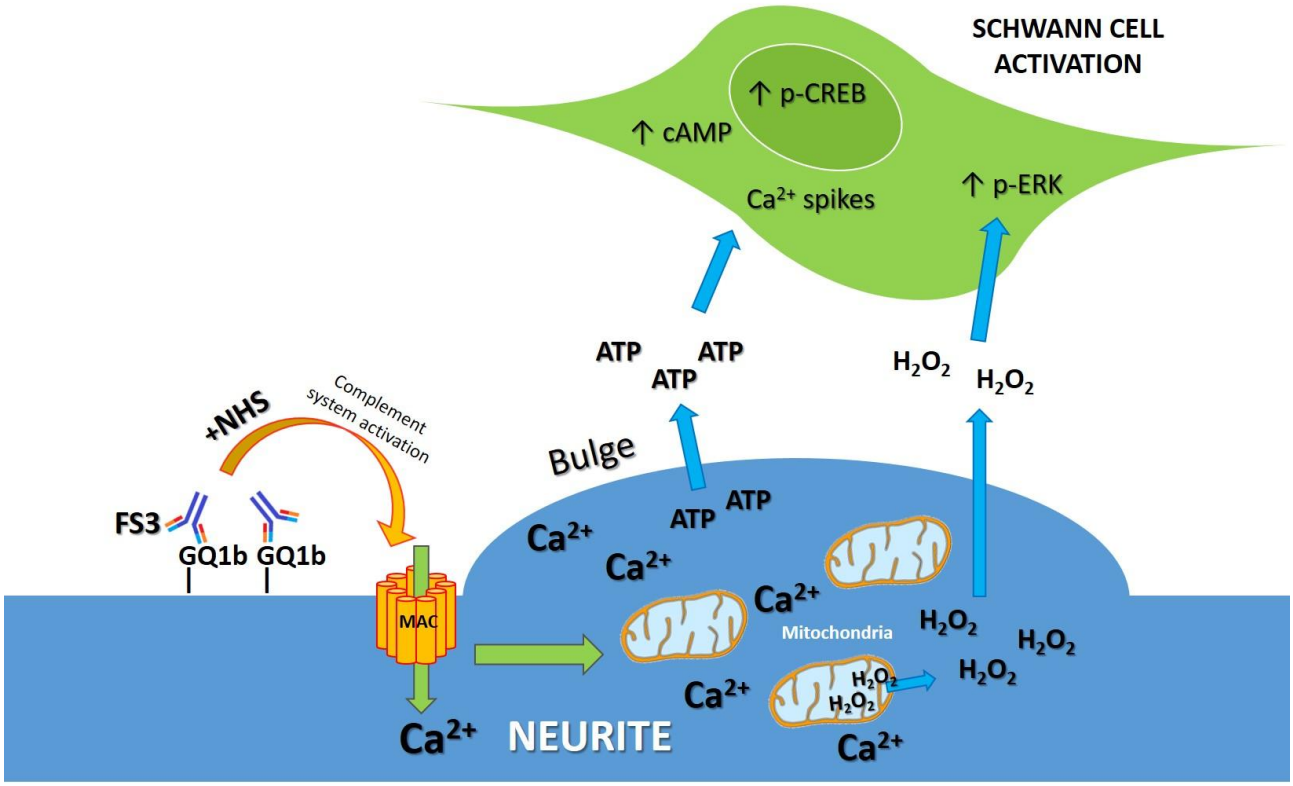

Figure 20: Hydrogen peroxide and ATP involvement in the signaling exchanged between the MAC-attacked neuron and Schwann cells. FS3 recruits and activates complement proteins provided by the NHS upon binding at GQ1b (or GT1a) gangliosides exposed at the plasma membrane of primary neurons. These events result in the insertion of MAC pore in the membrane bilayer and massive Ca^{2+} entry, which in turn leads to mitochondrial damage and formation of plasma membrane varicosities (bulges). The MAC damaged neuron releases hydrogen peroxide, derived from impaired electron transport chain in the mitochondria, and ATP in the extracellular enviroment. In response to these two *alarmins*, neighboring Schwann cells activate an array of intracellular responses, including ERK1/2 signaling pathway, the transcription factor CREB activity and second messengers Ca^{2+} and cAMP mediated pathways.

6. REFERENCES

(1) Love FM, Thompson WJ. Glial Cells Promote Muscle Reinnervation by Responding to Activity-Dependent Postsynaptic Signals. Journal of Neuroscience 1999;19(23):10390-10396.

(2) Jessen KR, Mirsky R, Lloyd AC. Schwann Cells : Development and Role in Nerve Repair. Cold Spring Harbor Perspectives in Biology 2015:1-16.

(3) Sugiura Y, Lin W. Neuron-glia interactions: the roles of Schwann cells in neuromuscular synapse formation and function. Biosci Rep 2011 10;31(5):295-302.

(4) Reddy LV, Koirala S, Sugiura Y, Herrera AA, Ko C. Glial Cells Mantain Synaptic Structure and Function and Promote Development of the Neuromuscular Junction In Vivo. Neuron 2003;40:563-580.

(5) Jahromi BS, Robitaille R, Charlton MP. Transmitter release increases intracellular calcium in perisynaptic Schwann cells in situ. Neuron 1992;8(6):1069-1077.

(6) Rochon D, Rousse I, Robitaille R. Synapse-glia interactions at the mammalian neuromuscular junction. The Journal of neuroscience : the official journal of the Society for Neuroscience 2001;21(11):3819-3829.

(7) Waller A. Experiments on the Section of the Glossopharyngeal and Hypoglossal Nerves of the Frog, and Observations of the Alterations Produced Thereby in the Structure of Their Primitive Fibres. Philosophical Transactions of the Royal Society of London 1850;140:423-429.

(8) Conforti L, Gilley J, Coleman MP. Wallerian degeneration: an emerging axon death pathway linking injury and disease. Nature Reviews Neuroscience 2014;15(6):394-409.

(9) Clemence A, Mirsky R, Jessen K. Non-myelin-forming Schwann cells proliferate rapidly during Wallerian degeneration in the rat sciatic nerve. J Neurocytol 1989;18(2):185-192.

(10) Thomson C, Griffiths I, McCulloch M, Kyriakides E, Barrie J, Montague P. In vitro studies of axonally-regulated Schwann cell genes during Wallerian degeneration. J Neurocytol 1993;22(8):590-602.

(11) Stoll G, Griffin J, Li CY, Trapp BD. Wallerian degeneration in the peripheral nervous system: participation of both Schwann cells and macrophages in myelin degradation. J Neurocytol 1989;18(5):671-683.

(12) Torigoe K, Tanaka H, Takahashi A, Awaya A, Hashimoto K. Basic behavior of migratory Schwann cells in peripheral nerve regeneration. Exp Neurol 1996;137(2):301-308.

(13) Kanda T. Biology of the blood-nerve barrier and its alteration in immune mediated neuropathies. J Neurol Neurosurg Psychiatr 2013;84(2):208-12.

(14) Brosius Lutz A, Barres BA. Contrasting the Glial Response to Axon Injury in the Central and Peripheral Nervous Systems. Developmental Cell 2014;28(1):7-17.

(15) Son YJ, Thompson WJ. Schwann cell processes guide regeneration of peripheral axons. Neuron 1995 01;14(1):125-32.

(16) Son YJ, Thompson WJ. Nerve sprouting in muscle is induced and guided by processes extended by Schwann cells. Neuron 1995 01;14(1):133-41.

(17) Georgiou J, Robitaille R, Trimble WS, Charlton MP. Synaptic regulation of glial protein expression in vivo. Neuron 1994;12(2):443-455.

(18) Duregotti E, Negro S, Scorzeto M, Zornetta I, Dickinson BC, Chang CJ. Mitochondrial alarmins released by degenerating motor axon terminals activate perisynaptic Schwann cells. PNAS 2015:1-9.

(19) Ushkaryov YA. alpha-Latrotoxin and Its Receptors. Handb Exp Pharmacol. Heidelberg; 2008;(184):171-206.

(20) Duchen LW, Gomez S, Queiroz LS. The neuromuscular junction of the mouse after black widow spider venom. J Physiol 1981 07;316:279-91.

(21) Plomp JJ, Molenaar PC, O'Hanlon GM, Jacobs BC, Veitch J, Daha MR, et al. Miller Fisher anti-GQ1b antibodies: alpha-latrotoxin-like effects on motor end plates. Ann Neurol 1999;45(2):189-199.

(22) Tedesco E, Rigoni M, Caccin P, Grishin E, Rossetto O, Montecucco C. Calcium overload in nerve terminals of cultured neurons intoxicated by alpha-latrotoxin and snake PLA2 neurotoxins. Toxicon: official journal of the International Society on Toxinology 2009 08;54(2):138-44.

(23) Duregotti E, Tedesco E, Montecucco C, Rigoni M. Calpains participate in nerve terminal degeneration induced by spider and snake presynaptic neurotoxins. Toxicon: official journal of the International Society on Toxinology 2013 03;64:20-8.

(24) Negro S, Bergamin E, Rodella U, Duregotti E, Scorzeto M, Jalink K, et al. ATP Released by Injured Neurons Activates Schwann Cells. Frontiers in Cellular Neuroscience 2016;10:1-8.

(25) Krysko DV, Agostinis P, Krysko O, Garg AD, Bachert C, Lambrecht BN, et al. Emerging role of damage-associated molecular patterns derived from mitochondria in inflammation. Trends Immunol 2011;32(4):157-164.

(26) Ydens E, Lornet G, Smits V, Goethals S, Timmerman V, Janssens S. The neuroinflammatory role of Schwann cells in disease. Neurobiol Dis 2013 07;55:95-103.

(27) Meyer zH, Hu W, Hartung H, Lehmann HC, Kieseier BC. The immunocompetence of Schwann cells. Muscle Nerve 2008 01;37(1):3-13.

(28) Tzekova N, Heinen A, Küry P. Molecules involved in the crosstalk between immune- and peripheral nerve schwann cells. J Clin Immunol 2014 07;34 Suppl 1:86-104.

(29) Dickinson BC, Chang CJ. Chemistry and biology of reactive oxygen species in signaling or stress responses. Nature chemical biology 2011;7(8):504-511.

(30) van der Vliet A, Janssen-Heininger YM. Hydrogen Peroxide as a Damage Signal in Tissue Injury and Inflammation: Murderer, Mediator, or Messenger? 2014;435:427-435.

(31) Napoli I, Noon La, Ribeiro S, Kerai AP, Parrinello S, Rosenberg LH, et al. A central role for the ERK-signaling pathway in controlling Schwann cell plasticity and peripheral nerve regeneration in vivo. Neuron 2012 03;73(4):729-42.

(32) Fields RD, Stevens-Graham B. New insights into neuron-glia communication. Science 2002 10;298(5593):556-62.

(33) Fields RD, Burnstock G. Purinergic signalling in neuron-glia interactions. Nat Rev Neurosci. 2006;7(6):423-36.

(34) Auld DS, Robitaille R. Perisynaptic Schwann Cells at the Neuromuscular Junction: Nerve- and Activity-Dependent Contributions to Synaptic Efficacy, Plasticity, and Reinnervation. Neuroscientist 2003;04;9(2):144-157.

(35) Vrbova G, Mehra N, Shanmuganathan H, Tyreman N, Schachner M, Gordon T. Chemical communication between regenerating motor axons and Schwann cells in the growth pathway. European Journal of Neuroscience 2009;30:366-375.

(36) O'Hanlon,G.M., Plomp JJ, Chakrabarti M, Morrison I, Wagner ER, Goodyear CS, et al. Anti-GQ1b ganglioside antibodies mediate complement-dependent destruction of the motor nerve terminal. Brain 2001 05;124:893-906.

(37) Guillain G, Barré J, Strohl A. Sur un syndrome de radiculo-névrite avec hyperalbuminose du liquide céphalo-rachidien sans réaction cellulaire. Remarques sur les caractèrescliniques et graphiques des réflexes tendineux. Bull Soc Méd Hôp Paris 1916;40:1462-70.

(38) Fisher M. An unusual variant of acute idiopathic polyneuritis (syndrome of ophthalmoplegia, ataxia and areflexia). N Engl J Med 1956;255(2):57-65.

(39) van den Berg B, Walgaard C, Drenthen J, Fokke C, Jacobs BC, Van Doorn PA. Guillain-Barré syndrome: pathogenesis, diagnosis, treatment and prognosis. Nature reviews Neurology 2014;10(8):469.

(40) Yuki N, Hartung H. Medical Progress Guillain-Barré Syndrome. N Engl J Med 2012:11-11.

(41) Willison HJ. The immunobiology of Guillain-Barré syndromes. Journal of Peripheral Nervous System 2005;112:94-112.

(42) McGrogan A, Madle GC, Seaman HE, De Vries CS. The epidemiology of Guillain-Barré syndrome worldwide: A systematic literature review. Neuroepidemiology 2009;32(2):150-163.

(43) Willison HJ, Goodyear CS. Glycolipid antigens and autoantibodies in autoimmune neuropathies. Trends Immunol 2013 09;34(9):453-9.

(44) Yuki N, Taki T, Inagaki F, Kasama T, Takahshi M, Saito K, et al. A bacterium lipopolysaccharide that elicits Guillain-Barré syndrome has a GM1 ganglioside-like structure. J Exp Med 1993;178:2-6.

(45) Yuki N, Susuki K, Koga M, Nishimoto Y, Odaka M, Hirata K, et al. Carbohydrate mimicry between human ganglioside GM1 and Campylobacter jejuni lipooligosaccharide causes Guillain-Barré syndrome. Proc Natl Acad Sci USA 2004.

(46) Koga M, Gilbert M, Li J, Koike S, Takahashi M, Furukawa K, et al. Antecedent infections in Fisher syndrome: a common pathogenesis of molecular mimicry. Neurology 2005 05;64(9):1605-11.

(47) Svennerholm L. Designation and schematic structure of gangliosides and allied glycosphingolipids. Prog Brain Res 1994 01;101:XI-XIV.

(48) Plomp JJ, Willison HJ. Pathophysiological actions of neuropathy-related anti-ganglioside antibodies at the neuromuscular junction. J Physiol (Lond) 2009 08;587:3979-99.

(49) Chiba A, Kusunoki S, Obata H, Machinami R, Kanazawa I. Serum anti-GQ1b IgG antibody is associated with ophthalmoplegia in Miller Fisher syndrome and Guillain-Barré syndrome: clinical and immunohistochemical studies. Neurology 1993;43(10):1911-1911.

(50) Willison HJ, O'Hanlon,G.M. The immunopathogenesis of Miller Fisher syndrome. J Neuroimmunol 1999 12;100(1-2):3-12.

(51) Liu J, Willison HJ, Pedrosa- Domellöf F. Immunolocalization of GQ1b and related gangliosides in human extraocular neuromuscular junctions and muscle spindles. Invest Ophthalmol Vis Sci 2009 07;50(7):3226-32.

(52) Carroll MV, Sim RB. Complement in health and disease. Adv Drug Deliv Rev 2011 09;63(12):965-75.

(53) Lovelace LL, Cooper CL, Sodetz JM, Lebioda L. Structure of Human C8 Protein Provides Mechanistic Insight into Membrane Pore Formation by Complement. Journal of biolo 2011;286(20):17585-17592.

(54) Serna M, Giles JL, Morgan BP, Bubeck D. Structural basis of complement membrane attack complex formation. Nature Communications 2016;7:1-22.

(55) Willison HJ, Plomp JJ. Anti-ganglioside antibodies and the presynaptic motor nerve terminal. Ann N Y Acad Sci 2008 01;1132:114-23.

(56) Halstead SK, O'Hanlon G,M., Humphreys PD, Morrison DB, Morgan BP, Todd AJ, et al. Anti-disialoside antibodies kill perisynaptic Schwann cells and damage motor nerve terminals via membrane attack complex in a murine model of neuropathy. Brain 2004 09;127:2109-23.

(57) Halstead SK, Humphreys PD, Goodfellow Ja, Wagner ER, Smith RaG, Willison HJ. Complement inhibition abrogates nerve terminal injury in Miller Fisher syndrome. Ann Neurol 2005 08;58(2):203-10.

(58) O'Hanlon G,M., Humphreys PD, Goldman RS, Halstead SK, Bullens RWM, Plomp JJ, et al. Calpain inhibitors protect against axonal degeneration in a model of anti-ganglioside antibody-mediated motor nerve terminal injury. Brain : a journal of neurology 2003 11;126:2497-509.

(59) Buchwald B, Zhang G, Vogt-Eisele A, Zhang W, Ahangari R, Griffin JW, et al. Anti-ganglioside antibodies alter presynaptic release and calcium influx. Neurobiol Dis 2007 10;28(1):113-121.

(60) Rigoni M, Pizzo P, Schiavo G, Weston AE, Zatti G, Caccin P, et al. Calcium influx and mitochondrial alterations at synapses exposed to snake neurotoxins or their phospholipid hydrolysis products. The Journal of biological chemistry 2007 04;282(15):11238-45.

(61) Rigoni M, Paoli M, Milanesi E, Caccin P, Rasola A, Bernardi P, et al. Snake phospholipase A2 neurotoxins enter neurons, bind specifically to mitochondria, and open their transition pores. The Journal of biological chemistry 2008 12;283(49):34013-20.

(62) Dickinson BC, Chang CJ. A targetable fluorescent probe for imaging hydrogen peroxide in the mitochondria of living cells. J Am Chem Soc 2008;130(30):9638-9639.

(63) Klarenbeek J, Goedhart J, Van Batenburg A, Groenewald D, Jalink K. Fourth-generation Epac-based FRET sensors for cAMP feature exceptional brightness, photostability and dynamic range: Characterization of dedicated sensors for FLIM, for ratiometry and with high affinity. PLoS ONE 2015;10(4):1-11.

(64) Halstead SK, Morrison I, O'Hanlon G,M., Humphreys PD, Goodfellow Ja, Plomp JJ, et al. Anti-disialosyl antibodies mediate selective neuronal or Schwann cell injury at mouse neuromuscular junctions. Glia 2005 11;52(3):177-89.

(65) Rupp A, Morrison I, Barrie Ja, Halstead SK, Townson KH, Greenshields KN, et al. Motor nerve terminal destruction and regeneration following anti-ganglioside antibody and complement-mediated injury: an in and ex vivo imaging study in the mouse. Exp Neurol 2012 02;233(2):836-48.

(66) Angaut-Petit D, Molgo J, Connold AL, Faille L. The levator auris longus muscle of the mouse: a convenient preparation for studies of short-and long-term presynaptic effects of drugs or toxins. Neurosci Lett 1987;82(1):83-88.

(67) Fewou SN, Rupp A, Nickolay LE, Carrick K, Greenshields KN, Pediani J, et al. Anti-ganglioside antibody internalization attenuates motor nerve terminal injury in a mouse model of acute motor axonal neuropathy. J Clin Invest 2012;122(3):1037-1051.

(68) Cunningham ME, McGonigal R, Meehan GR, Barrie JA, Yao D, Halstead SK, et al. Anti-ganglioside antibodies are removed from circulation in mice by neuronal endocytosis. Brain 2016 06: 139(Pt 6):1657-65.

(69) Mallon BS, Shick HE, Kidd GJ, Macklin WB. Proteolipid promoter activity distinguishes two populations of NG2-positive cells throughout neonatal cortical development. J Neurosci 2002 Feb 1;22(3):876-885.

(70) Brill MS, Lichtman JW, Thompson W, Zuo Y, Misgeld T. Spatial constraints dictate glial territories at murine neuromuscular junctions. J Cell Biol 2011 Oct 17;195(2):293-305.

(71) Levi G, Aloisi F, Ciotti M, Gallo V. Autoradiographic localization and depolarization-induced release of acidic amino acids in differentiating cerebellar granule cell cultures. Brain Res 1984;290(1):77-86.

(72) Arce V, Garces A, de Bovis B, Filippi P, Henderson C, Pettmann B, et al. Cardiotrophin-1 requires LIFRβ to promote survival of mouse motoneurons purified by a novel technique. J Neurosci Res 1999;55(1):119-126.

(73) Diebolder Ca, Beurskens FJ, de Jong R,N., Koning RI, Strumane K, Lindorfer Ma, et al. Complement is activated by IgG hexamers assembled at the cell surface. Science 2014 03;343(6176):1260-3.

(74) Riboni L, Prinetti a, Pitto M, Tettamanti G. Patterns of endogenous gangliosides and metabolic processing of exogenous gangliosides in cerebellar granule cells during differentiation in culture. Neurochem Res 1990 12;15(12):1175-83.

(75) Thangnipon W, Balázs R. Developmental changes in gangliosides in cultured cerebellar granule neurons. Neurochem Res 1992 01;17(1):45-59.

(76) Aureli M, Loberto N, Lanteri P, Chigorno V, Prinetti A, Sonnino S. Cell surface sphingolipid glycohydrolases in neuronal differentiation and aging in culture. J Neurochem 2011 03;116(5):891-9.

(77) Yi M, Weaver D, Hajnóczky G. Control of mitochondrial motility and distribution by the calcium signal: A homeostatic circuit. J Cell Biol 2004;167(4):661-672.

(78) Rizzuto R, De Stefani D, Raffaello A, Mammucari C. Mitochondria as sensors and regulators of calcium signalling. Nature reviews Molecular cell biology 2012;13(9):566-578.

(79) Rasola A, Bernardi P. Mitochondrial permeability transition in Ca^{2+}-dependent apoptosis and necrosis. Cell Calcium 2011;50(3):222-233.

(80) Giorgio V, von Stockum S, Antoniel M, Fabbro A, Fogolari F, Forte M, et al. Dimers of mitochondrial ATP synthase form the permeability transition pore. Proc Natl Acad Sci USA 2013 Apr 9;110(15):5887-5892.

(81) Paulsen CE, Carroll KS. Orchestrating redox signaling networks through regulatory cysteine switches. ACS chemical biology 2010 01;5(1):47-62.

(82) Miller EW, Dickinson BC, Chang CJ. Aquaporin-3 mediates hydrogen peroxide uptake to regulate downstream intracellular signaling. Proc Natl Acad Sci USA 2010 Sep 7;107(36):15681-15686.

(83) Bienert GP, Chaumont F. Aquaporin-facilitated transmembrane diffusion of hydrogen peroxide. Biochimica et Biophysica Acta 2014;1840(5):1596-1604.

(84) Gough D, Cotter T. Hydrogen peroxide: a Jekyll and Hyde signalling molecule. Cell death & disease 2011;2(10):e213.

(85) Murphy MP, Holmgren A, Larsson N, Halliwell B, Chang CJ, Kalyanaraman B, et al. Unraveling the biological roles of reactive oxygen species. Cell metabolism 2011;13(4):361-366.

(86) Tabernero A, Stewart HJ, Jessen KR, Mirsky R. The Neuron-Glia Signal β Neuregulin Induces Sustained CREB Phosphorylation on Ser-133 in Cultured Rat Schwann Cells. Molecular and Cellular Neuroscience 1998;10(5):309-322.

(87) Valdez G, Tapia JC, Lichtman JW, Fox MA, Sanes JR. Shared resistance to aging and ALS in neuromuscular junctions of specific muscles. PloS one 2012;7(4):e34640.

(88) Mayer M. Development of the one-hit theory of immune hemolysis. Immunochemical Approaches to Problems in Microbiology 1961:268-279.

(89) Cooper ST, Mcneil PL. Membrane repair: mechanisms and pathophysiology. Physiol Rev 2015(178):1205-1240.

(90) Morgan BP, Campbell AK. The recovery of human polymorphonuclear leucocytes from sublytic complement attack is mediated by changes in intracellular free calcium. Biochem J 1985;231:205-208.

(91) Morgan BP. Complement membrane attack recovery and non-lethal effects nucleated cells: resistance, recovery and non-lethal effects. Biochem J 1989;264:1-14.

(92) Fields RD, Ni Y. Nonsynaptic Communication Through ATP Release from Volume-Activated Anion Channels in Axons. Neuroscience 2010;3(142):1-15.

(93) Abe MK, Kartha S, Karpova AY, Li J, Liu PT, Kuo W, et al. Hydrogen peroxide activates extracellular signal-regulated kinase via protein kinase C, Raf-1, and MEK1. American journal of respiratory cell and molecular biology 1998;18(4):562-569.

(94) Crossthwaite AJ, Hasan S, Williams RJ. Hydrogen peroxide-mediated phosphorylation of ERK1/2, Akt/PKB and JNK in cortical neurones: dependence on Ca^{2+} and PI3-kinase. J Neurochem 2002;80(1):24-35.

(95) Harrisingh MC, Perez-Nadales E, Parkinson DB, Malcolm DS, Mudge AW, Lloyd AC. The Ras/Raf/ERK signalling pathway drives Schwann cell dedifferentiation. EMBO J 2004 Aug 4;23(15):3061-3071.

(97) Pryzwansky KB, Kidao S, Merricks EP. Compartmentalization of PDE-4 and cAMP-dependent protein kinase in neutrophils and macrophages during phagocytosis. Cell Biochem Biophys 1998;28(2-3):251-275.

(98) Shaywitz AJ, Greenberg ME. CREB: a stimulus-induced transcription factor activated by a diverse array of extracellular signals. Annu Rev Biochem 1999;68(1):821-861.

7. APPENDICES

7.1 List of Abbreviations

Ach	Acetylcholine
AchRs	Acetylcholine receptors
AGAbs	Anti-ganglioside antibodies
AMAN	Acute motor axonal neuropathy
AMP	Adenosine monophosphate
ATP	Adenosine triphosphate
BNB	Blood-nerve barrier
BSA	Bovine serum albumine
cAMP	Cyclic adenosine monophosphate
CFP	Cyan fluorescent protein
CGNs	Cerebellar granular neurons
CNS	Central nervous system
CREB	cAMP response element-binding protein
DAMPs	Damage-associated molecular patterns
DIV	Days in vitro
EJPs	Evoked junction potentials
EOMs	Extraocular muscles
EPPs	Evoked action potentials
FCCP	Carbonyl cyanide-p-trifluoromethoxyphenylhydrazone
FRET	Fluorescence Resonance Energy Transfer
GBS	Guillain-Barré syndrome
GFP	Green Fluorescent Protein
HI-NHS	Heat-inactivated normal human serum
HRP	Horseradish peroxidase
Hz	Hertz
IgG	Immunoglobulin G
IgM	Immunoglobulin M
LAL	Levator auris longus
LDH	Lactate dehydrogenase
LOS	Lipo-oligosaccharide
LPS	Lipo-polysaccharide
MAC	Membrane attack complex
MAT	Motor axon terminal
MEPPs	Miniature postsynaptic potentials
MF	Muscle fibre
MFS	Miller Fisher syndrome
NF	Neurofilaments
NHS	Normal human serum

NMJ	Neuromuscular junction
PBS	Phosphate buffered saline
PF6-AM	Peroxyfluor 6 acetoxymethyl ester
PFA	Paraformaldehyde
PNS	Peripheral nervous system
PRRs	Pattern recognition receptors
PSCs	Perisynaptic Schwann cells
ROI	Region of interest
ROS	Reactive oxygen species
RT	Room temperature
SCMNs	Spinal cord motor neurons
SCs	Schwann cells
TLRs	Toll-like Receptors
TMRM	Tetramethylrhodamine methyl ester
VAchT	Vescicular Acetylcholine Transporter
YFP	Yellow fluorescent protein
α-BTx	α-bungarotoxin
α-LTX	α-Latrotoxin

7.2 List of publications

- **Rodella U**, Negro S, Scorzeto M, Bergamin E, Jalink K, Montecucco C, Yuki N, Rigoni M (**2017**). *Schwann cells are activated by ATP released from neurons in an in vitro cellular model of Miller Fisher syndrome*. Disease Models and Mechanisms, Epub ahead of print.

- **Rodella U**, Scorzeto M, Duregotti E, Negro S, Dickinson BC, Chang CJ, Yuki N, Rigoni M, Montecucco C (**2016**). *An animal model of Miller Fisher syndrome: Mitochondrial hydrogen peroxide is produced by the autoimmune attack of nerve terminals and activates Schwann cells.* Neurobiology of Disease, 96, 95-104.

- Negro S, Bergamin, E, **Rodella U**, Duregotti E, Scorzeto M, Jalink K, Montecucco C, Rigoni M (**2016**). *ATP Released by Injured Neurons Activates Schwann Cells.* Frontiers in Cellular Neuroscience, 10, 1–8.

7.3 Supplemetary Movies

Note: supplementary movies of: [Rodella E, et al. (2016) An animal model of Miller Fisher syndrome: Mitochondrial hydrogen peroxide is produced by the autoimmune attack of nerve terminals and activates Schwann cells. Neurobiol. Dis.] are available at: http://www.sciencedirect.com/science/article/pii/S0969996116302212